US007687937B2

(12) United States Patent
Lasseter et al.

(10) Patent No.: US 7,687,937 B2

(45) Date of Patent: Mar. 30, 2010

(54) CONTROL OF SMALL DISTRIBUTED ENERGY RESOURCES

(75) Inventors: **Robert H. Lasseter**, Madison, WI (US); **Paolo Piagi**, Woburn, MA (US)

(73) Assignee: **Wisconsin Alumni Research Foundation**, Madison, WI (US)

(*) Notice: Subject to any disclaimer, the term of this patent is extended or adjusted under 35 U.S.C. 154(b) by 861 days.

(21) Appl. No.: **11/084,737**

(22) Filed: **Mar. 18, 2005**

(65) **Prior Publication Data**

US 2006/0208574 A1 Sep. 21, 2006

(51) **Int. Cl.**
H02J 3/00 (2006.01)

(52) **U.S. Cl.** **307/69**; 307/65

(58) **Field of Classification Search** 307/65, 307/69

See application file for complete search history.

(56) **References Cited**

U.S. PATENT DOCUMENTS

5,041,959	A	8/1991	Walker	
5,329,222	A	7/1994	Gyugyi et al.	
5,596,492	A	1/1997	Divan et al.	
5,614,770	A	3/1997	Suelzle	
5,745,356	A	4/1998	Tassitino, Jr. et al.	
6,111,764	A	8/2000	Atou et al.	
6,188,205	B1	2/2001	Tanimoto et al.	
6,219,591	B1	4/2001	Vu et al.	
6,219,623	B1	4/2001	Wills	
6,249,411	B1	6/2001	Hemena et al.	
6,252,310	B1	6/2001	Wilhelm	
6,285,917	B1	9/2001	Sekiguchi et al.	
6,288,456	B1	9/2001	Cratty	
6,347,027	B1	2/2002	Nelson et al.	
6,356,471	B1	3/2002	Fang	
6,359,423	B1	3/2002	Noro	
6,465,910	B2	10/2002	Young et al.	
6,738,692	B2 *	5/2004	Schienbein et al.	700/286
6,870,279	B2	3/2005	Gilbreth et al.	
2003/0036806	A1	2/2003	Schienbein et al.	

OTHER PUBLICATIONS

DOE News, The DER Weekly, vol. 2, No. 10, Mar. 9, 2001, pp. 1-4.

Robert Lasseter, et al., "Integration of Distributed Energy Resources The CERTS MicroGrid Concept," Consortium for Electric Reliability Technology Solutions, Apr. 2002, pp. 1-27.

(Continued)

Primary Examiner—Albert W Paladini
Assistant Examiner—Hal I Kaplan
(74) *Attorney, Agent, or Firm*—Foley & Lardner LLP

(57) **ABSTRACT**

A method of controlling the output inverter of a microsource in a distributed energy resource system is disclosed. Embodiments of the invention include using unit or zone power controllers that reduce the operating frequency of the inverter to increase its unit output power. Preferred embodiments includes methods wherein the inverter reaches maximum output power and minimum operating frequency at the same time, and further comprising using a voltage controller implementing a voltage vs. reactive current droop. Other aspects of this embodiment relate to an inverter that implements such methods, and a microsource containing such an inverter. These methods can be extended to control inverters in a plurality of microsources, organized in a single zone or in a plurality of zones.

27 Claims, 25 Drawing Sheets

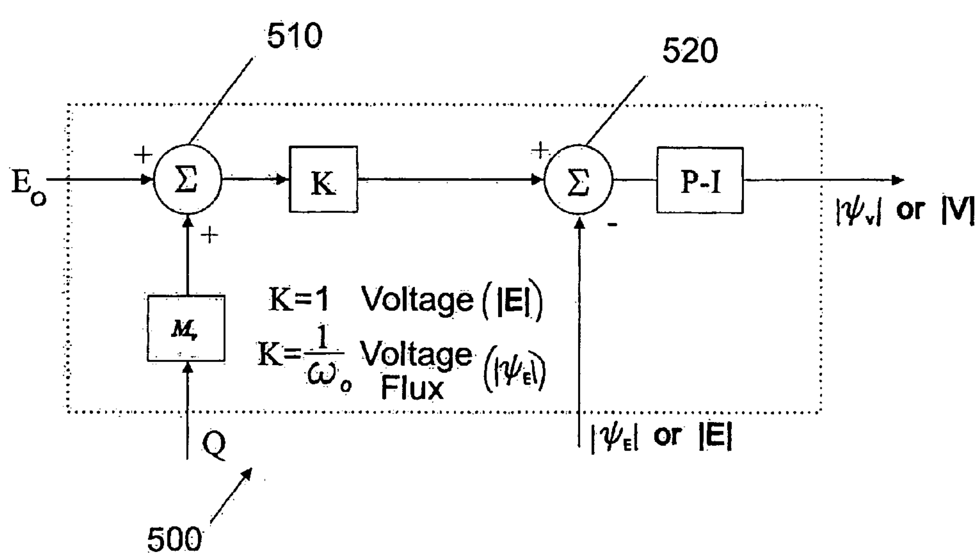

OTHER PUBLICATIONS

R.H. Lasseter, "MicroGrids," IEEE, No. 0-7803-7322, Jul. 2002, pp. 305-308.

Robert Lasseter, et al., "Scenarios for Distributed Technology Applications with Steady State and Dynamic Models of Loads and Micro-Sources," Consortium for Electric Reliability Technology Solutions, Apr. 14, 2000.

Robert Lasseter, et al., "Microgrid Proof of Concept," presented Jun. 2001, at Consortium for Electric Reliability Technology Solutions.

Friedman, N.R. "Distributed Energy Resources Interconnection Systems: Technology Review and Research Needs", National Renewable Energy Laboratory, Sep. 2002).

"1547 IEEE Standard for Interconnecting Distributed Resources with Electric Power Systems", Institute of Electrical and Electronics Engineers, Standards Coordinating Committee 21, Jul. 28, 2003 (http://ieeexplore.ieee.org/ie15/8676/27496/01225051.pdf?isnumber=27496&prod=STD&arnumber=1225051&arST=+16&arAuthor=, visited Jan. 14, 2008.

* cited by examiner

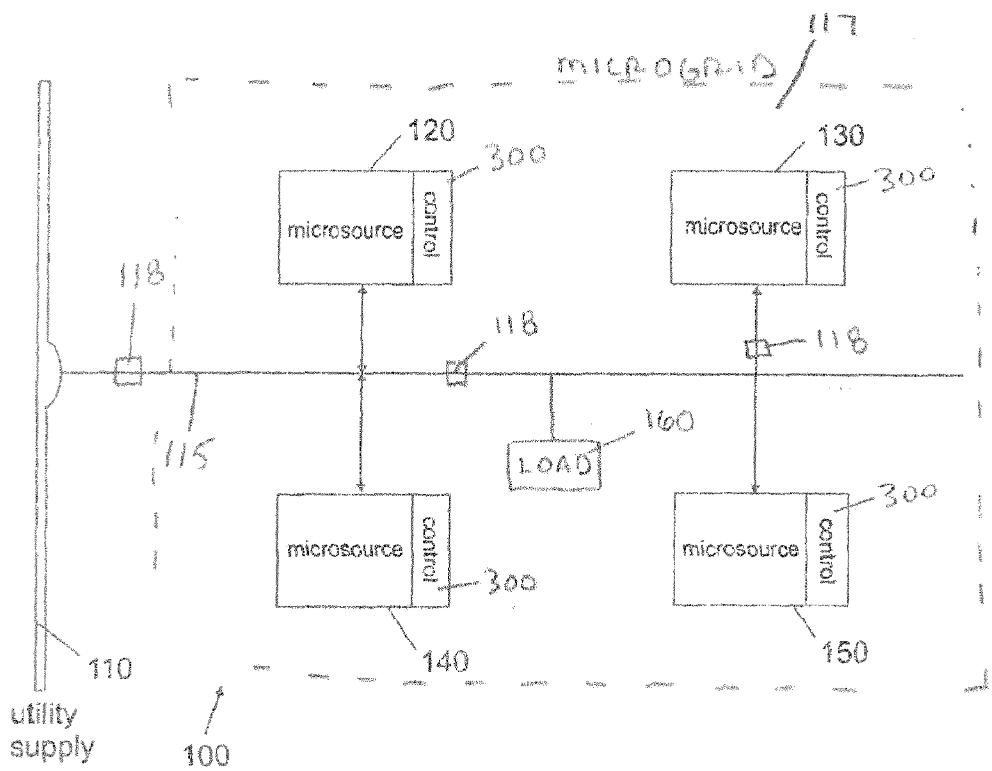

FIG. 1 (PRIOR ART)

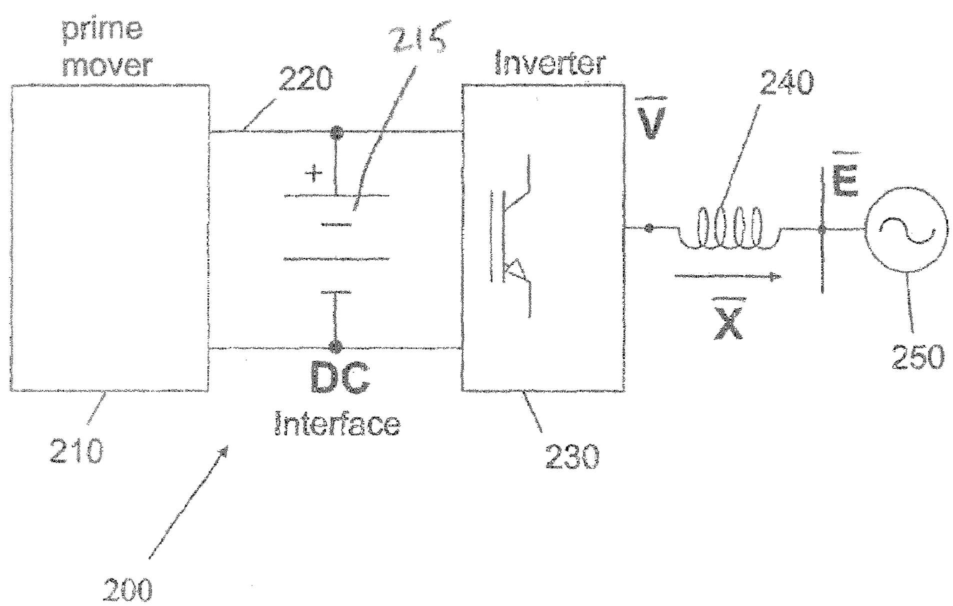

FIG. 2 (PRIOR ART)

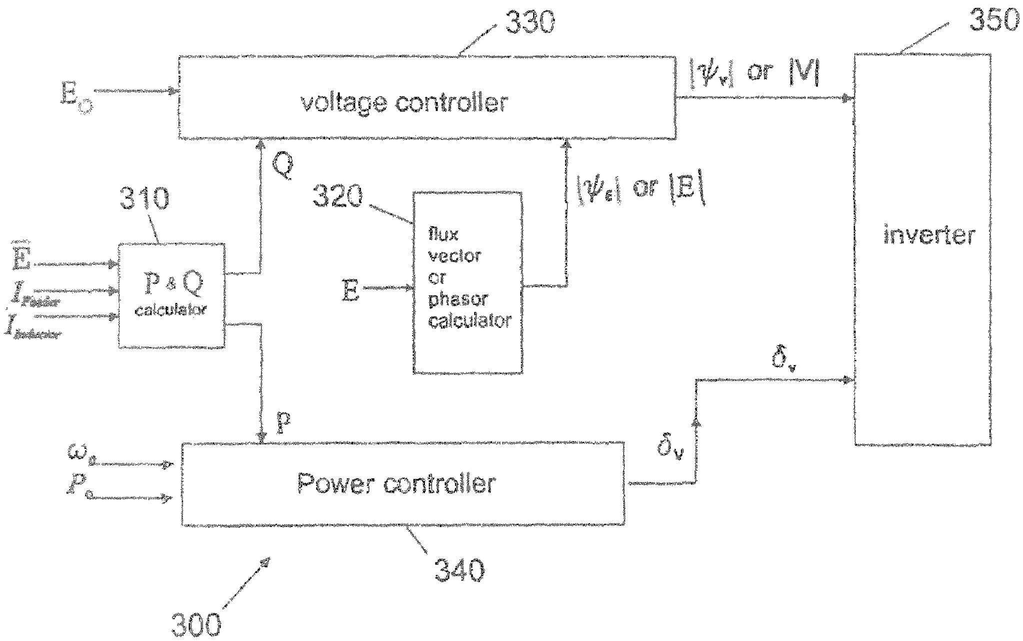

FIG. 3 (PRIOR ART)

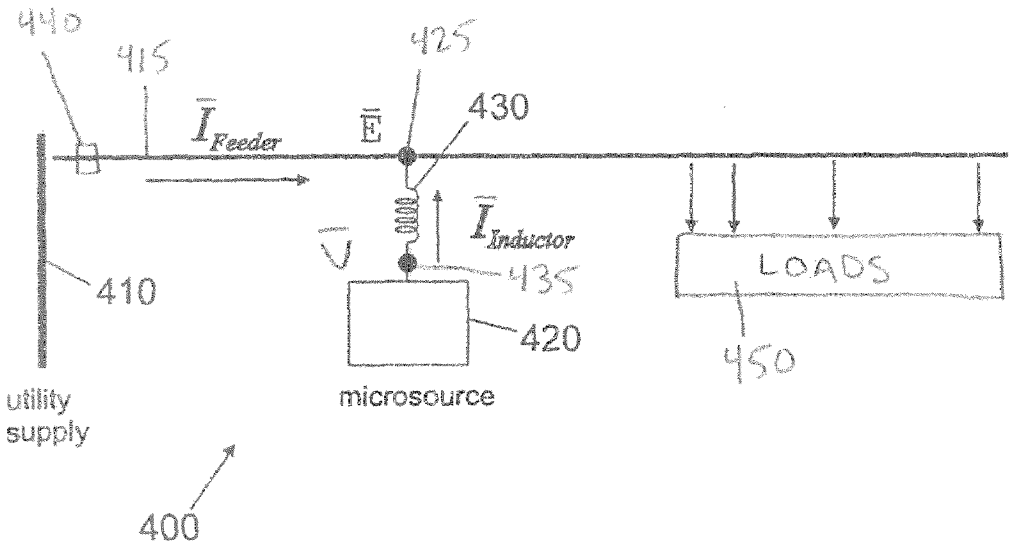

FIG. 4 (PRIOR ART)

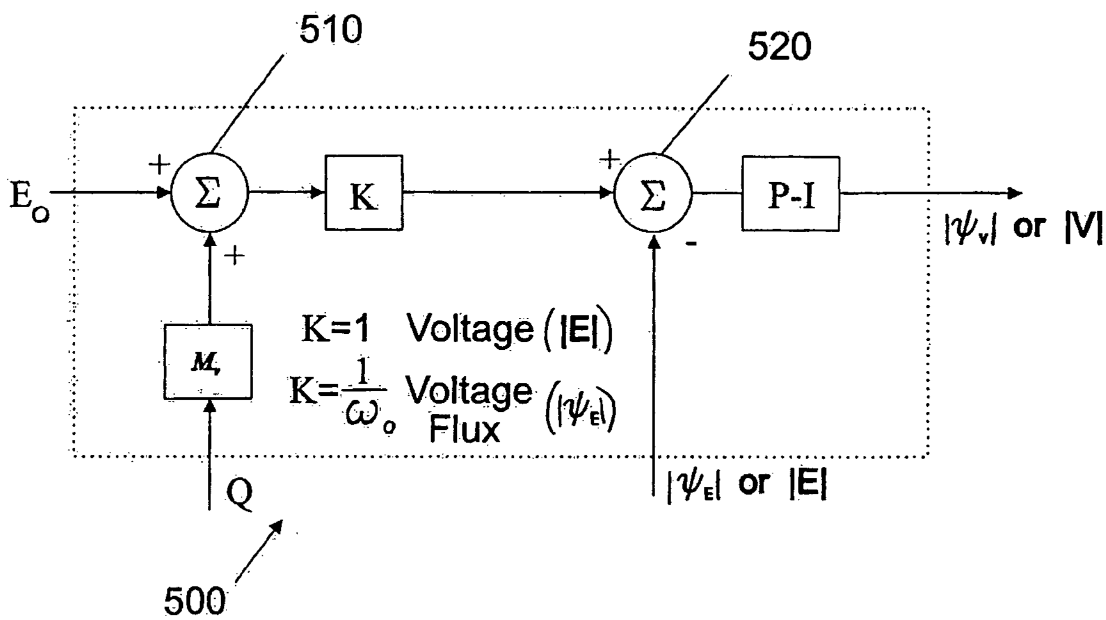
510
520
E
O
+
Σ
K
+
Σ
P-I
+
-
|ψv| or |V|
M
K=1 Voltage (|E|)
K=1/ωo Voltage Flux (|ψE|)
Q
|ψE| or |E|
500

FIG. 5

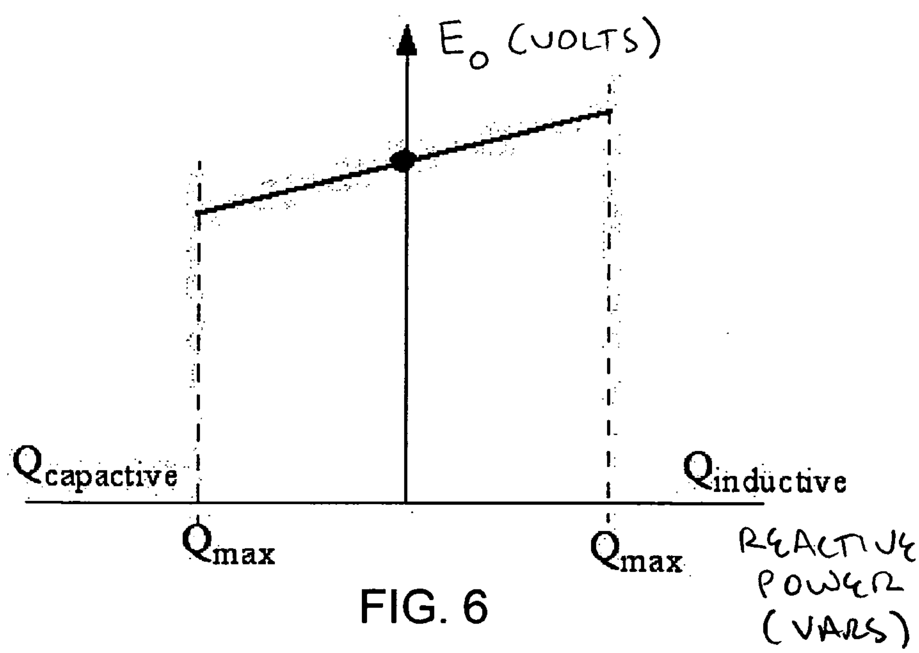
Eo (VOLTS)
Qcapactive
Qinductive
Qmax
Qmax
REACTIVE POWER (VARS)

FIG. 6

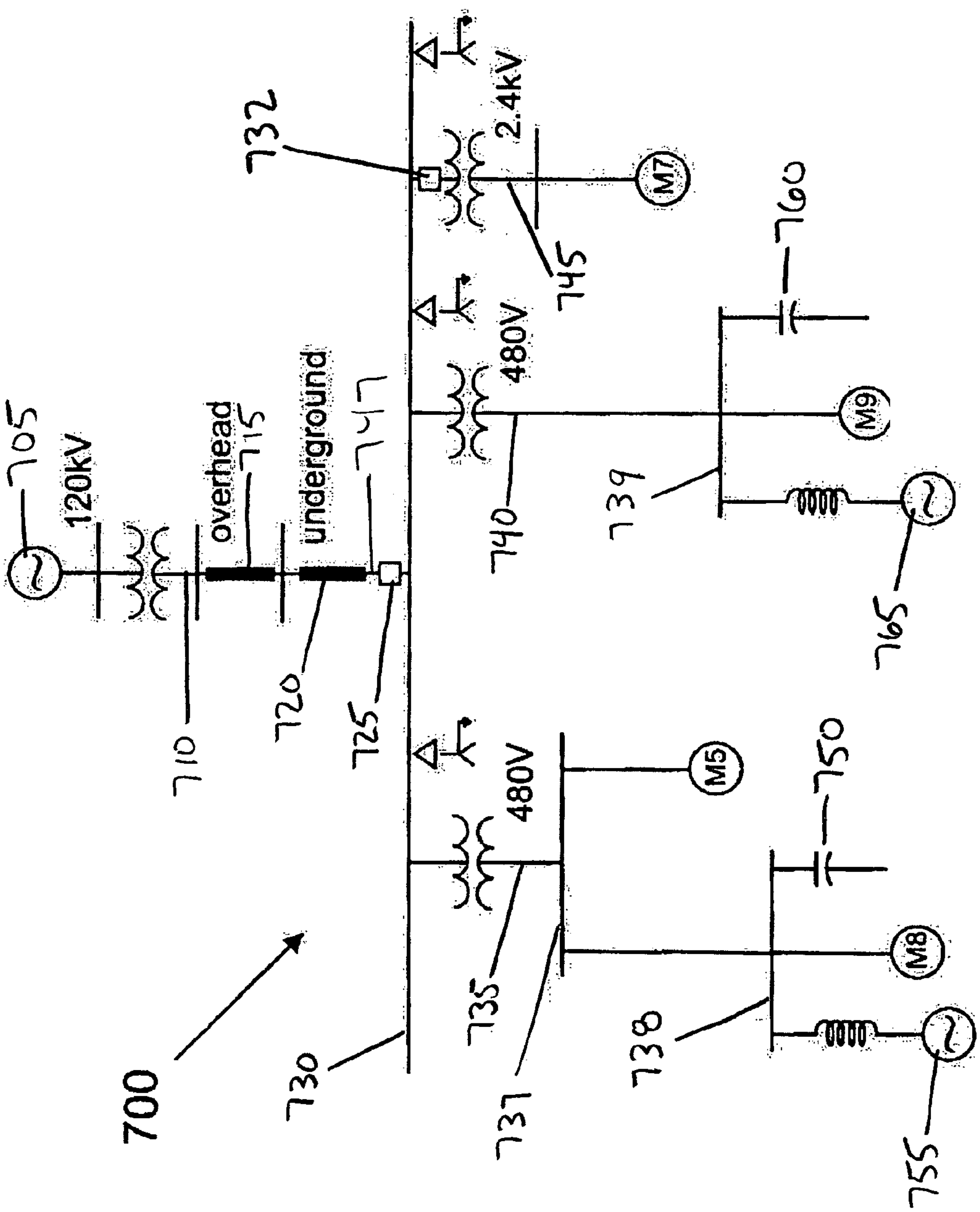
700
705
120kV
710
overhead
715
underground
720
747
725
730
731
732
735
480V
480V
2.4kV
738
739
740
745
750
755
760
765
M5
M7
M8
M9

FIG. 7

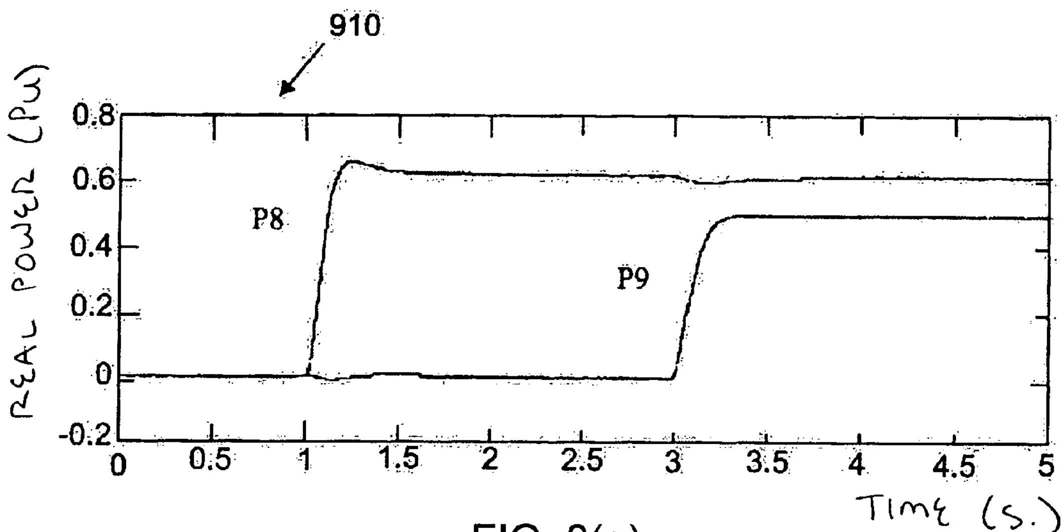
910
REAL POWER (PU)
0.8
0.6
0.4
0.2
0
-0.2
P8
P9
0
0.5
1
1.5
2
2.5
3
3.5
4
4.5
5
TIME (S.)

FIG. 8(a)

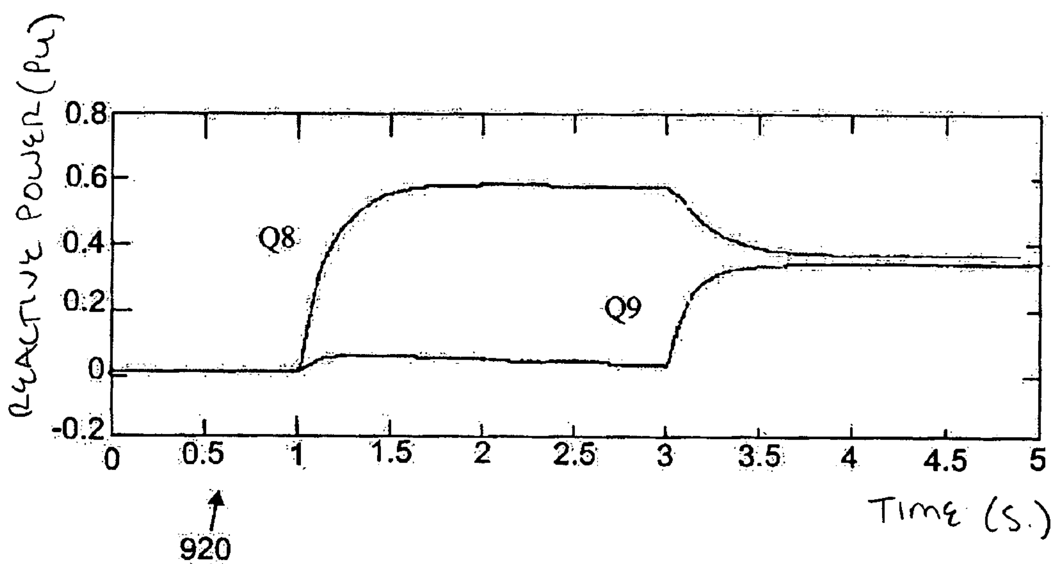
REACTIVE POWER (PU)
0.8
0.6
0.4
0.2
0
-0.2
Q8
Q9
0
0.5
1
1.5
2
2.5
3
3.5
4
4.5
5
TIME (S.)
920

FIG. 8(b)

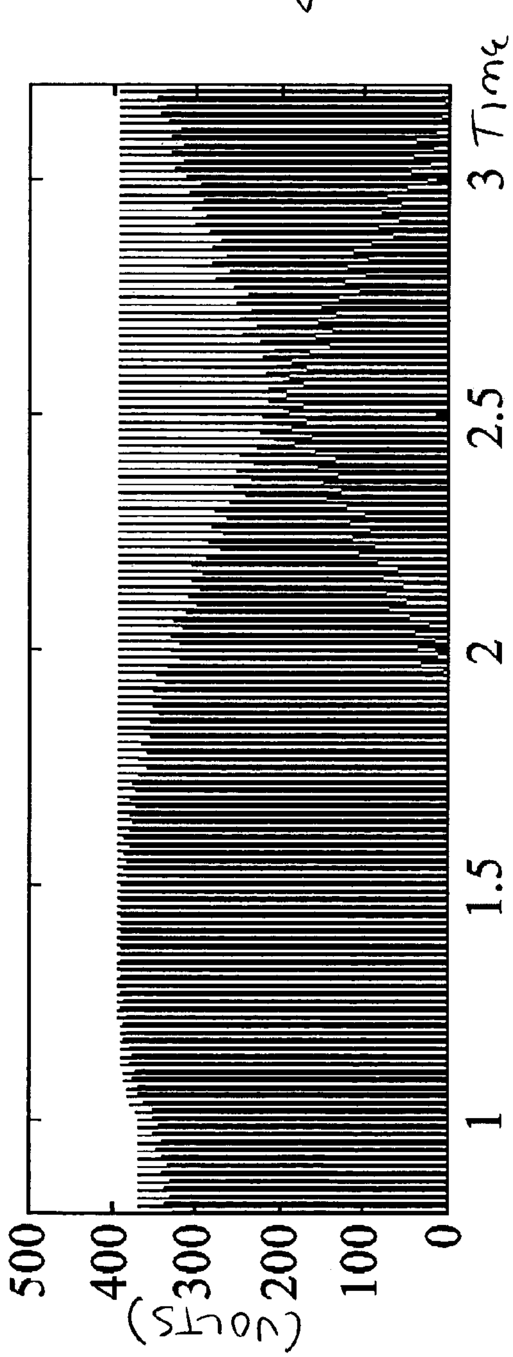
930
500
400
300
200
100
0
(VOLTS)
1
1.5
2
2.5
3
Time (s.)

FIG. 9(a)

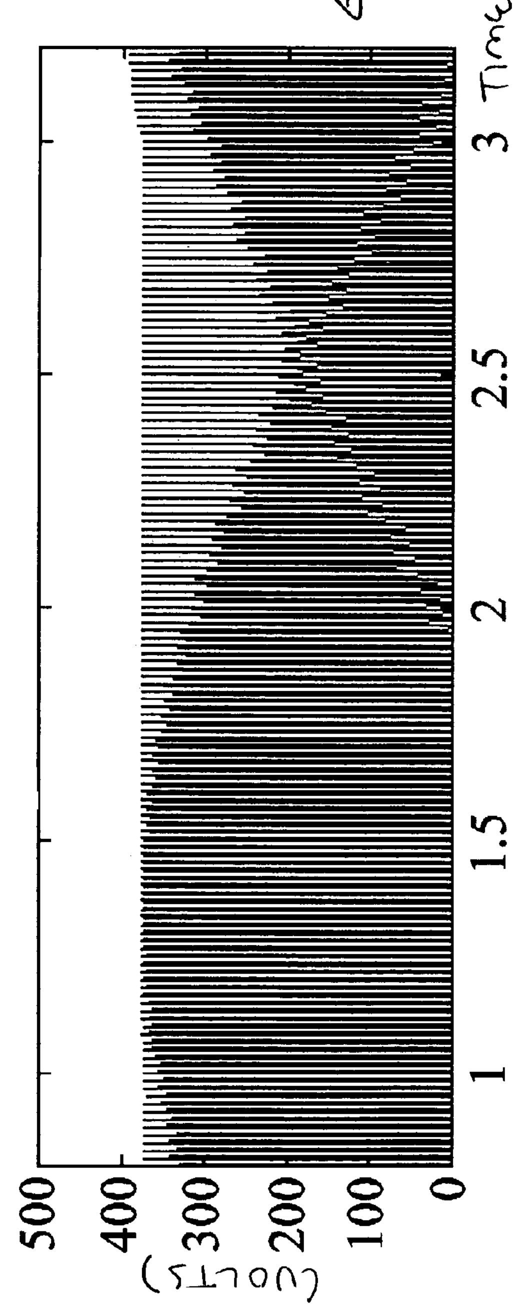
940
500
400
300
200
100
0
(VOLTS)
1
1.5
2
2.5
3
Time (s)

FIG. 9(b)

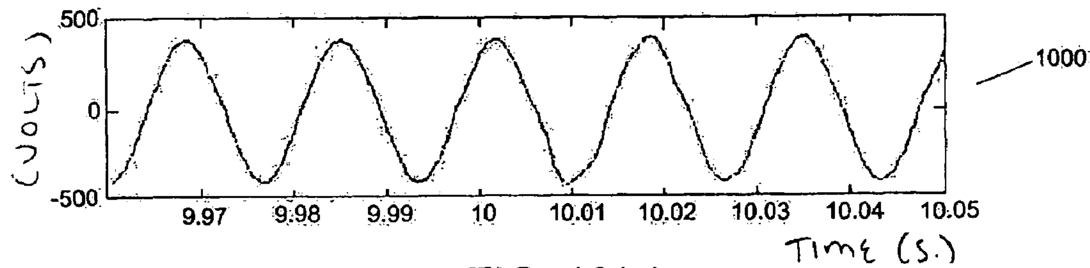

FIG. 10(a)

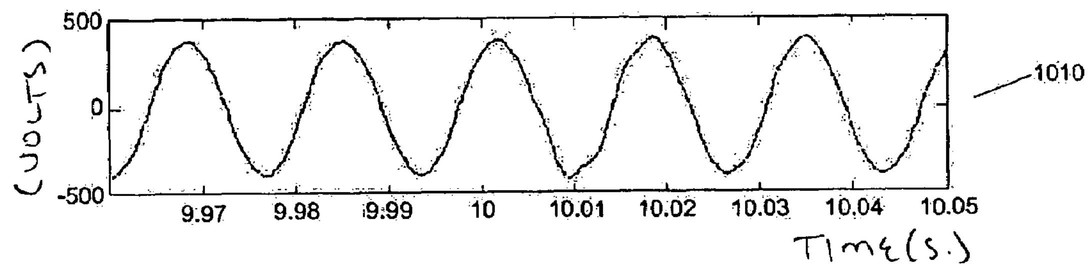

FIG. 10(b)

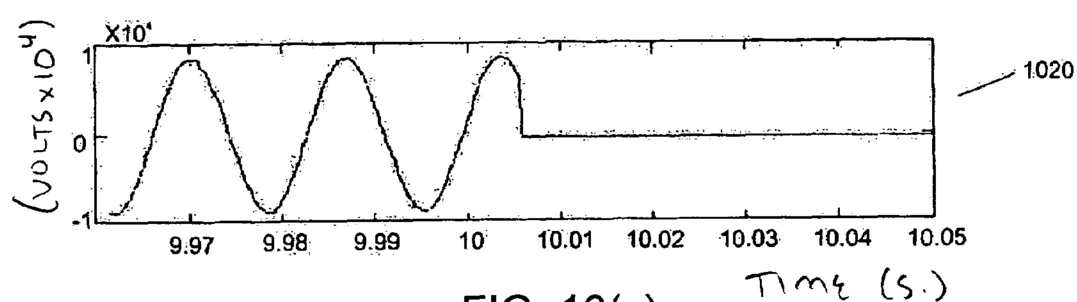

FIG. 10(c)

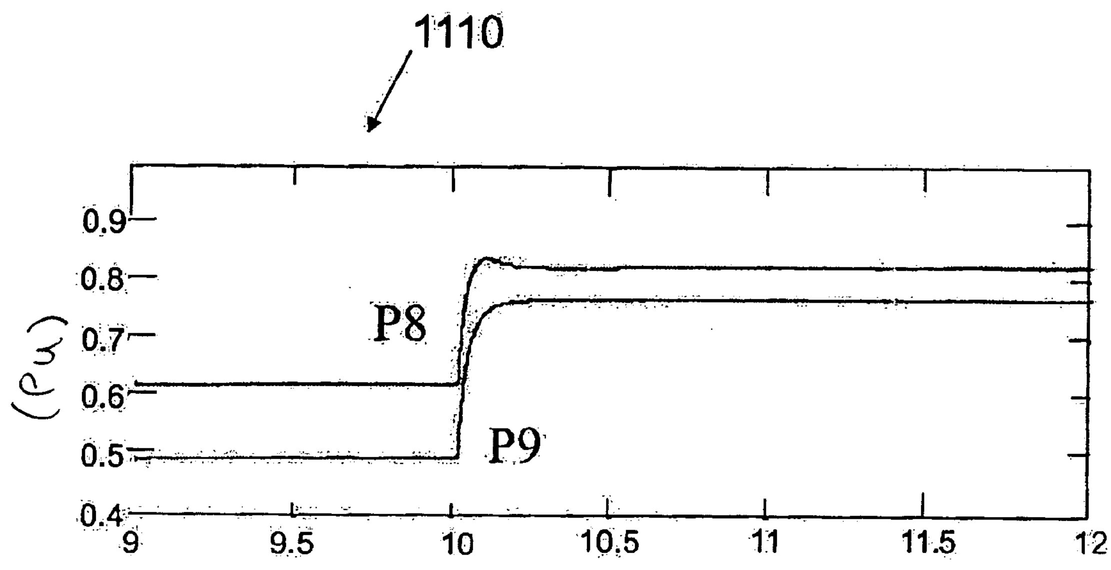

FIG. 11(a)

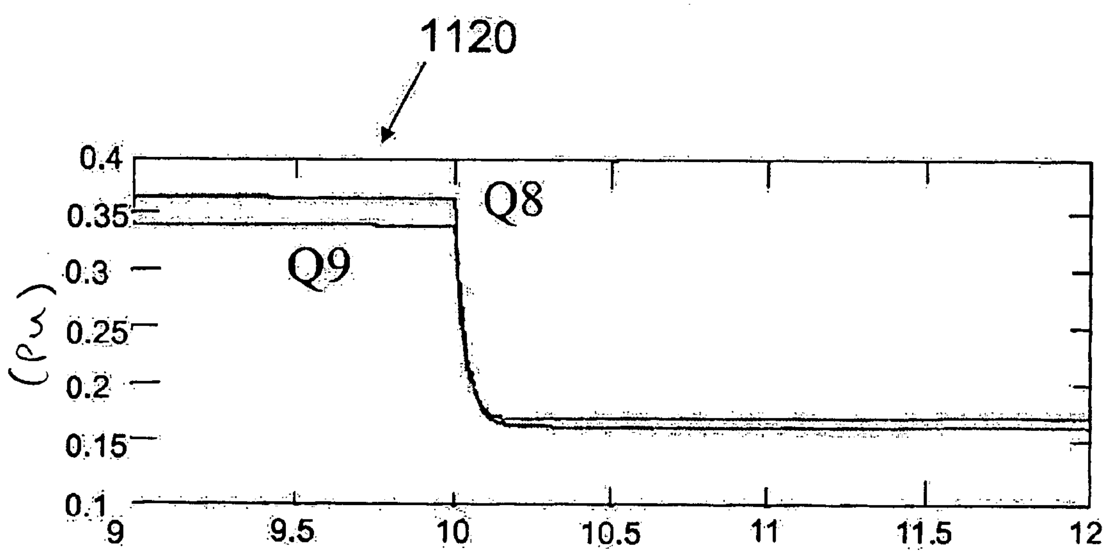

FIG. 11(b)

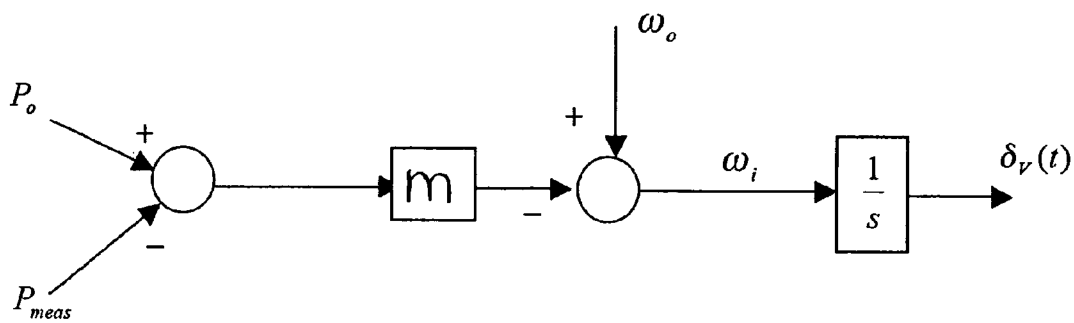

ω_o
P_o
+
+
m
−
ω_i
1/s
$\delta_V(t)$
−
P_{meas}

FIG. 12

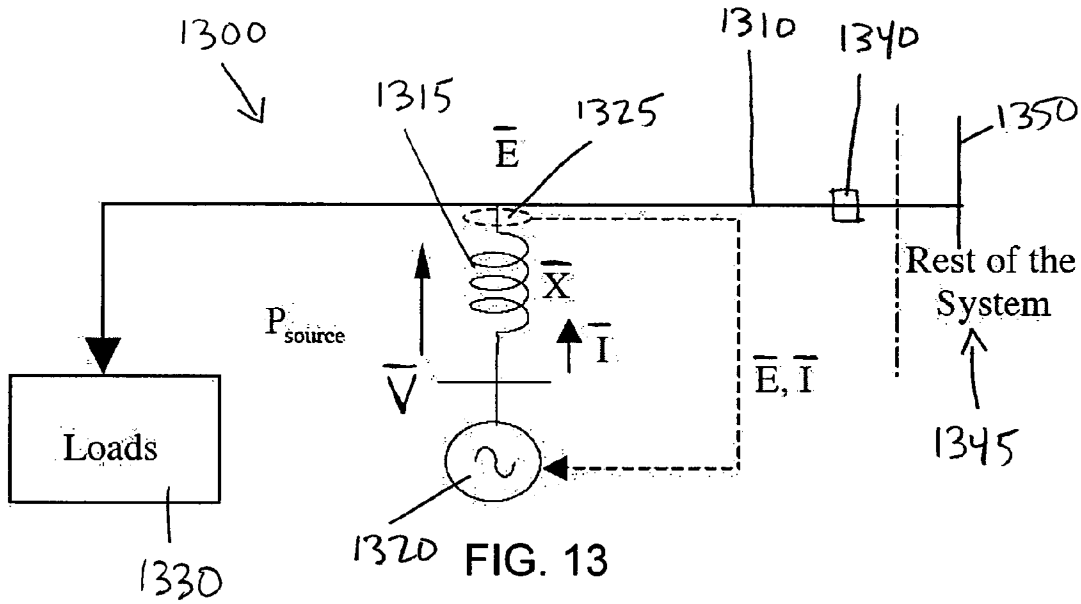

1300
1310
1340
1315
1325
1350
E
X
Rest of the System
P_{source}
I
V
E, I
Loads
1345
1330
1320

FIG. 13

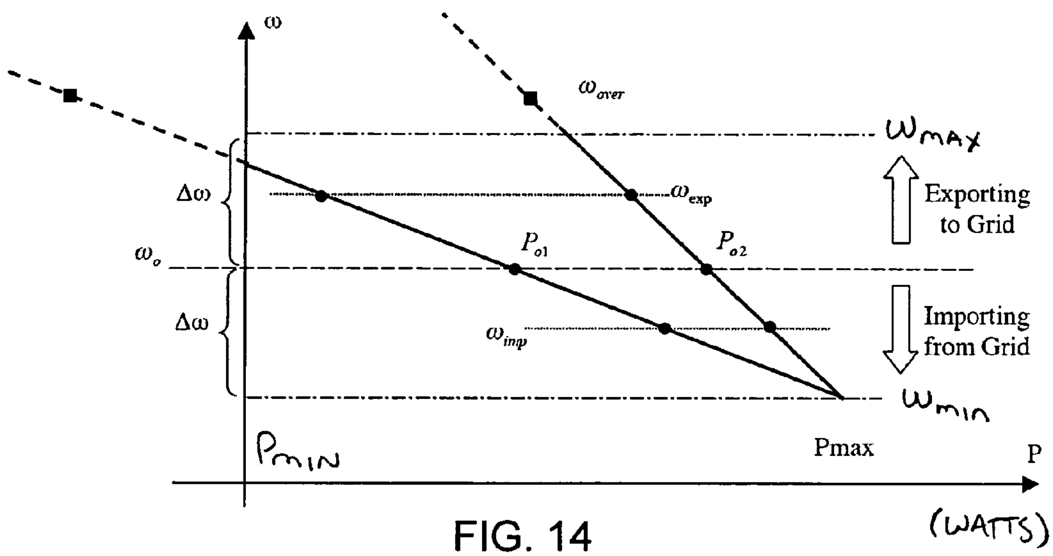
ω
ω_{over}
Wmax
Δω
ω_{exp}
Exporting to Grid
P_{o1}
P_{o2}
ω_o
Δω
Importing from Grid
ω_{imp}
Wmin
Pmin
Pmax
P
(WATTS)

FIG. 14

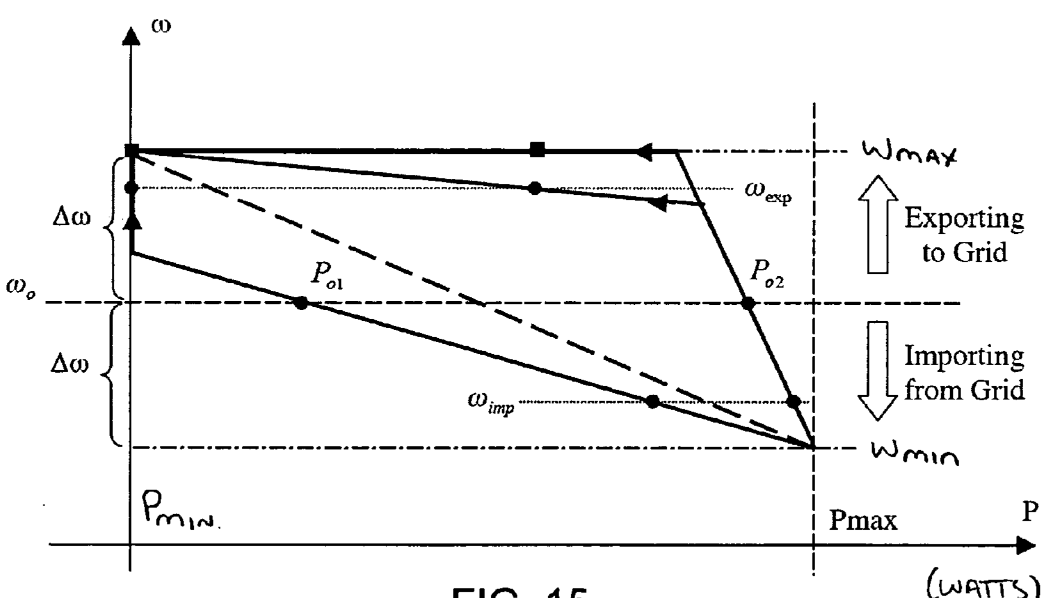
ω
Wmax
ω_{exp}
Δω
Exporting to Grid
P_{o1}
P_{o2}
ω_o
Δω
Importing from Grid
ω_{imp}
Wmin
Pmin.
Pmax
P
(WATTS)

FIG. 15

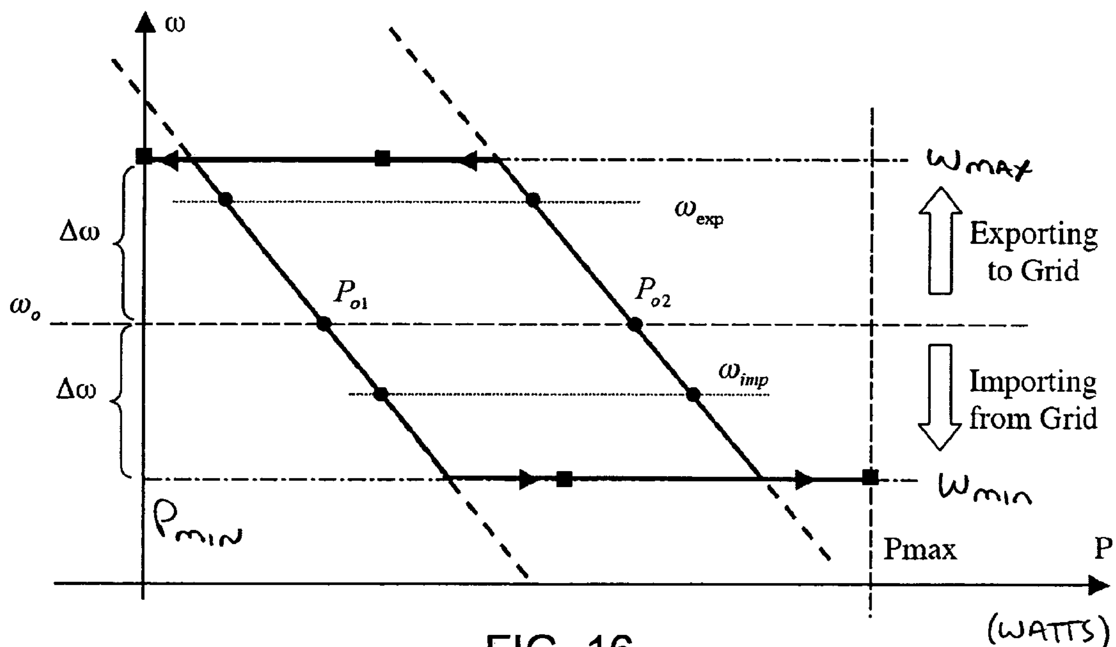

ω
ωmax
ωexp
Δω
Exporting to Grid
ωo
Po1
Po2
ωimp
Δω
Importing from Grid
ωmin
Pmin
Pmax
P
(WATTS)

FIG. 16

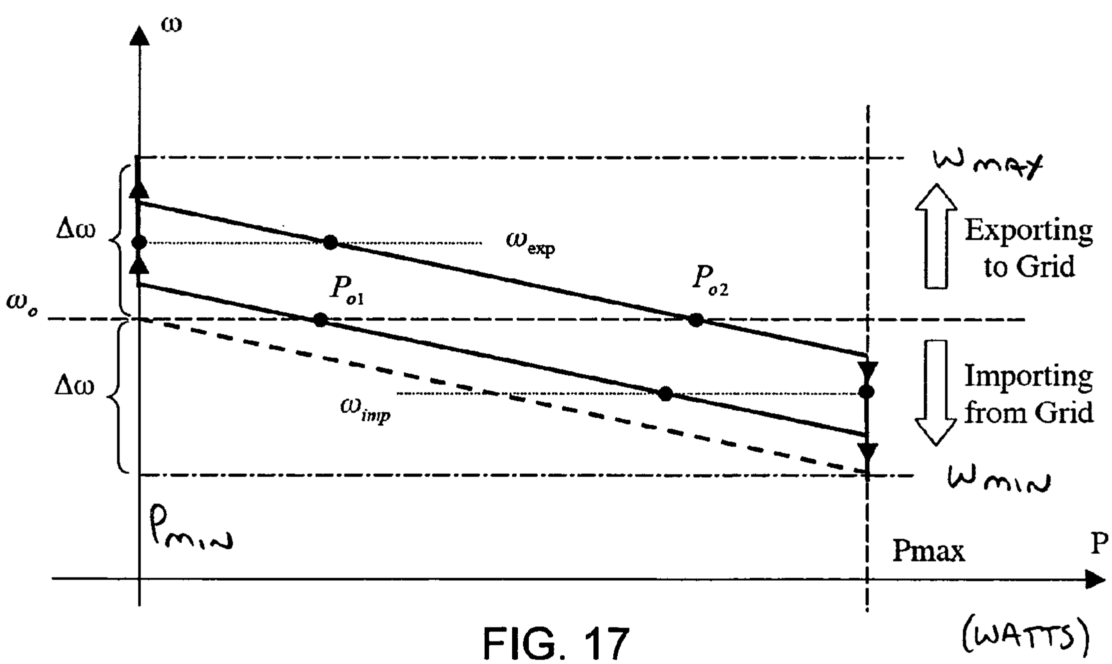

ω
ωmax
Δω
ωexp
Exporting to Grid
ωo
Po1
Po2
Δω
Importing from Grid
ωimp
ωmin
Pmin
Pmax
P
(WATTS)

FIG. 17

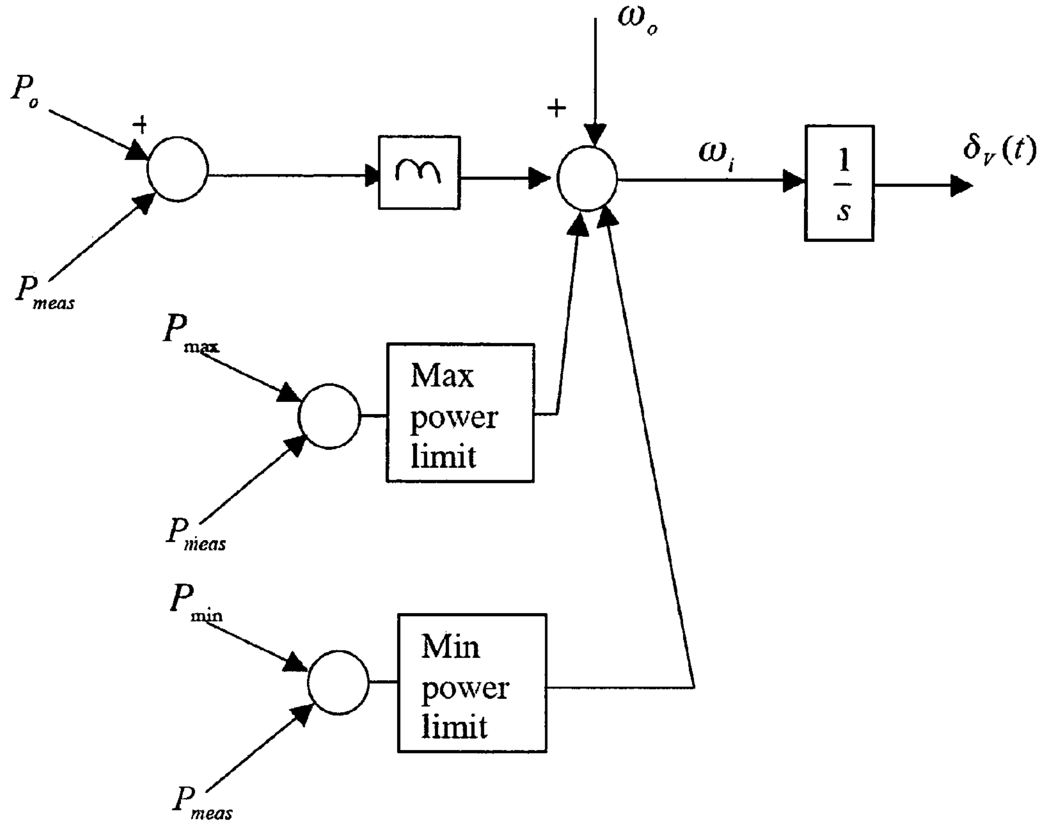

ω_o
P_o
+
+
m
ω_i
$\frac{1}{s}$
$\delta_V(t)$
P_{meas}
P_{max}
Max power limit
P_{meas}
P_{min}
Min power limit
P_{meas}

FIG. 18

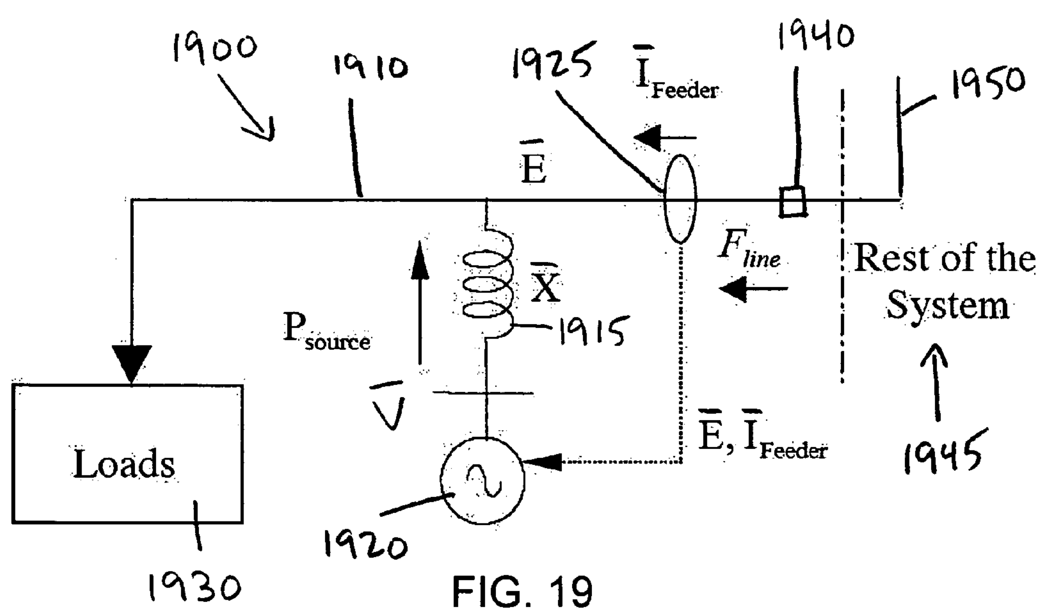

1900
1910
1925
$\bar{I}_{Feeder}$
1940
1950
$\bar{E}$
F_{line}
Rest of the System
$\bar{X}$
1915
P_{source}
$\bar{V}$
$\bar{E}, \bar{I}_{Feeder}$
1945
Loads
1920
1930

FIG. 19

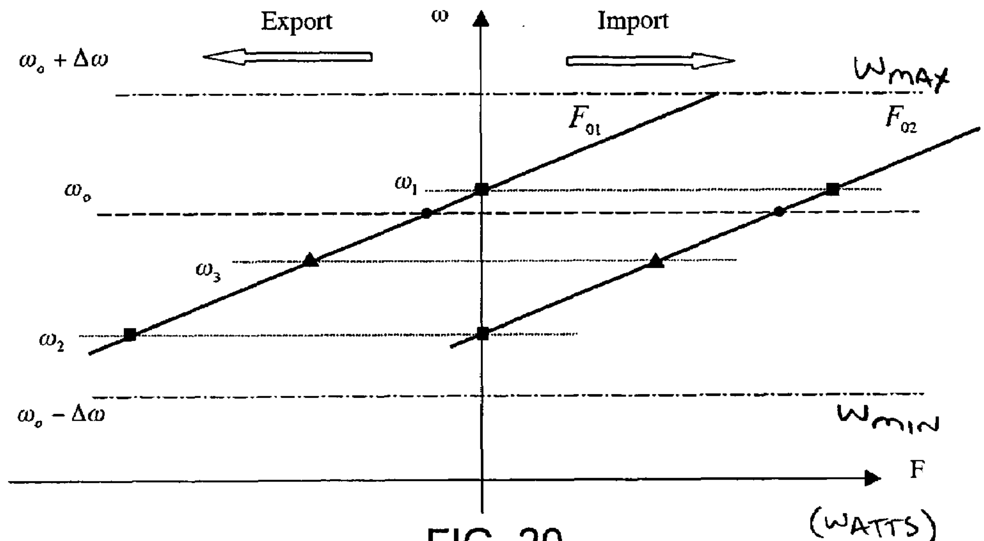

FIG. 20

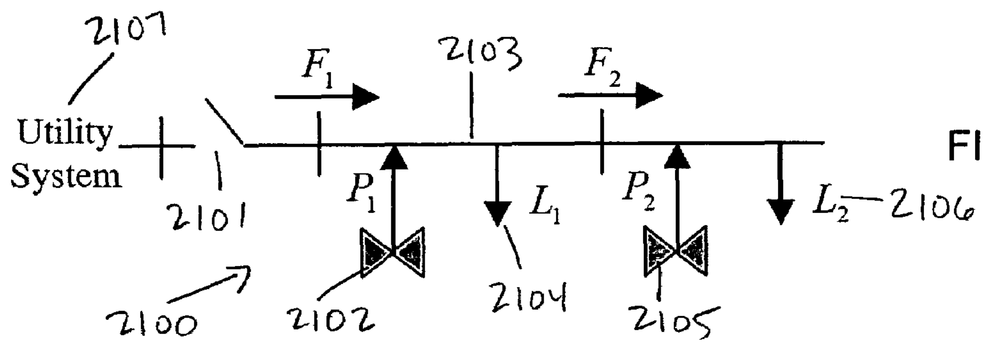

FIG. 21

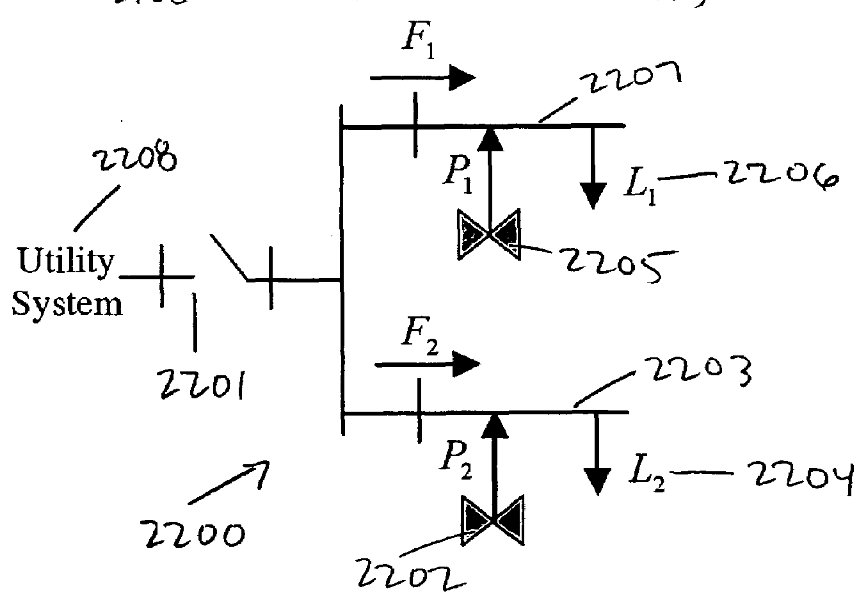

FIG. 22

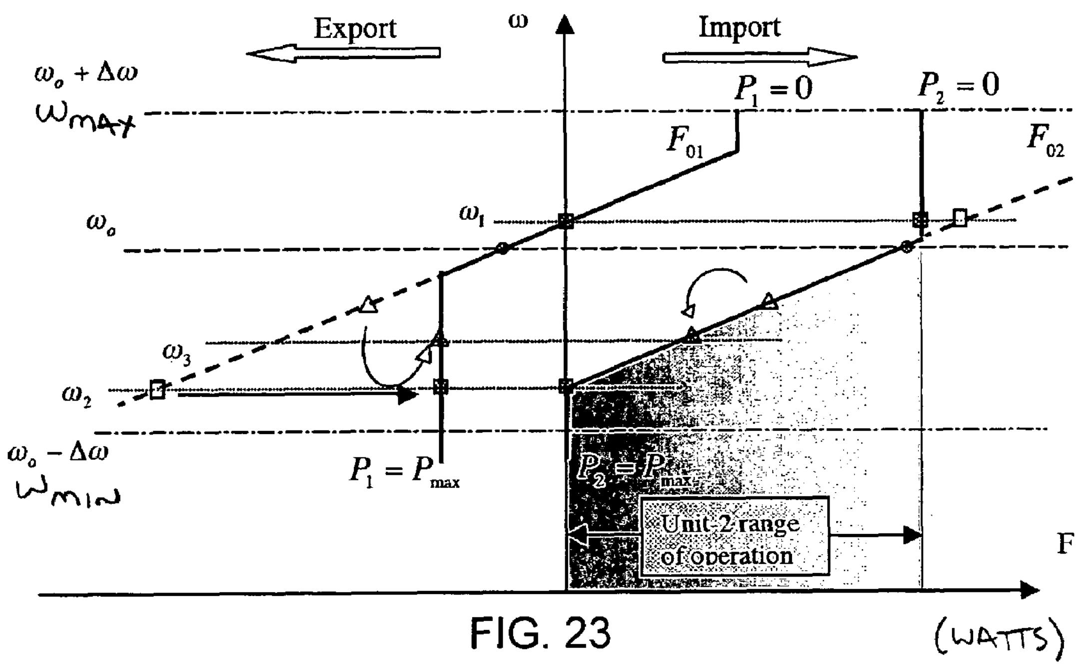
Export
ω
Import
ω_o + Δω
ω_MAX
P_1 = 0
P_2 = 0
F_01
F_02
ω_1
ω_o
ω_3
ω_2
ω_o − Δω
ω_MIN
P_1 = P_max
P_2 = P_max
Unit-2 range of operation
F
(WATTS)

FIG. 23

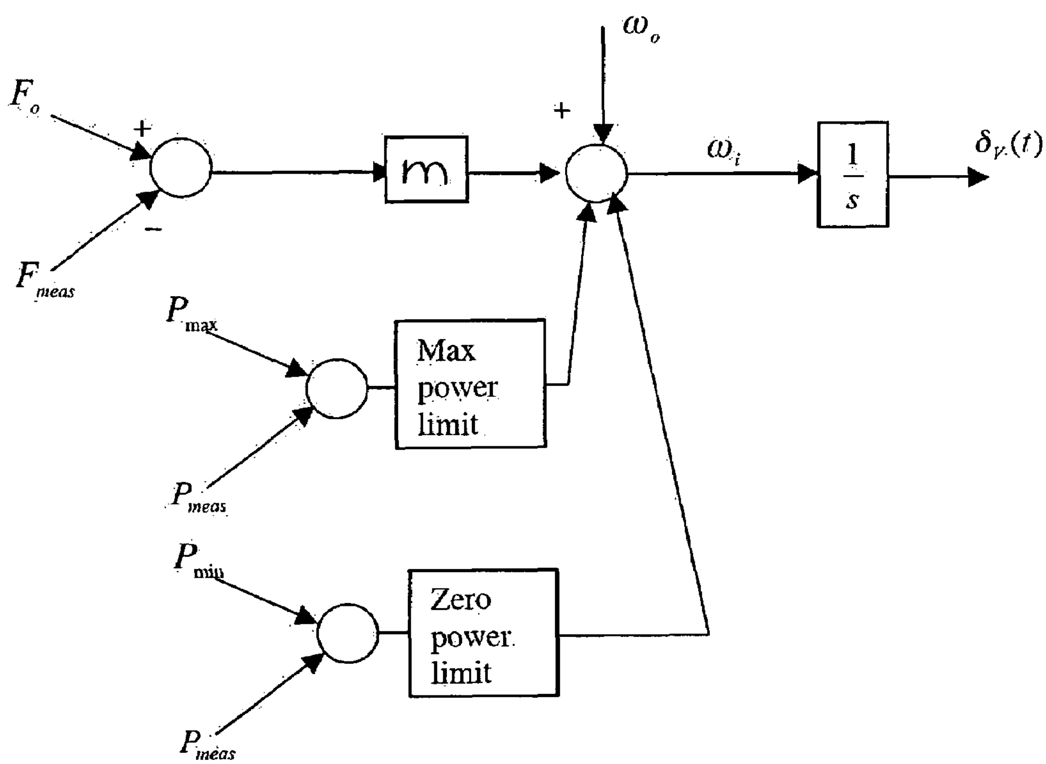
ω_o
F_o
+
−
F_meas
m
+
ω_i
1/s
δ_V(t)
P_max
Max power limit
P_meas
P_min
Zero power limit
P_meas

FIG. 24

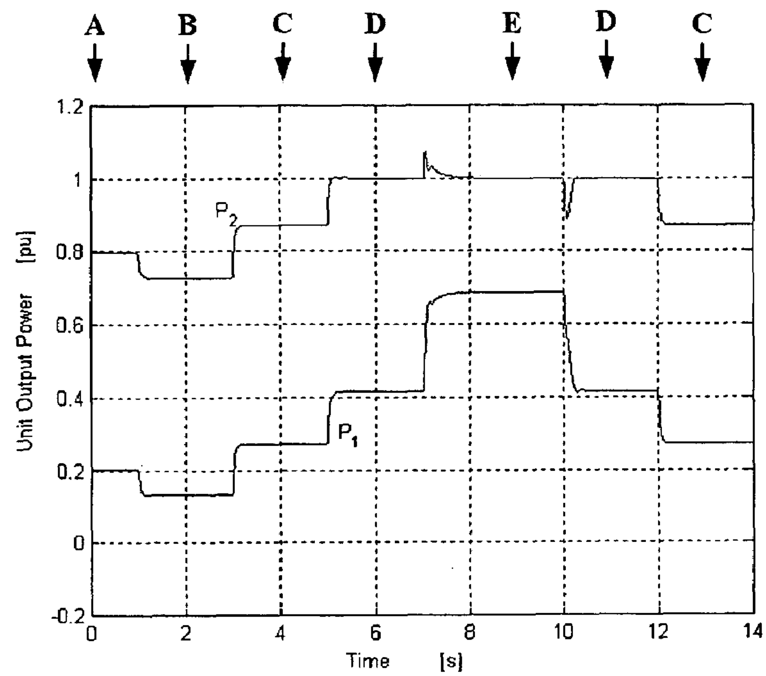

FIG. 25(a)

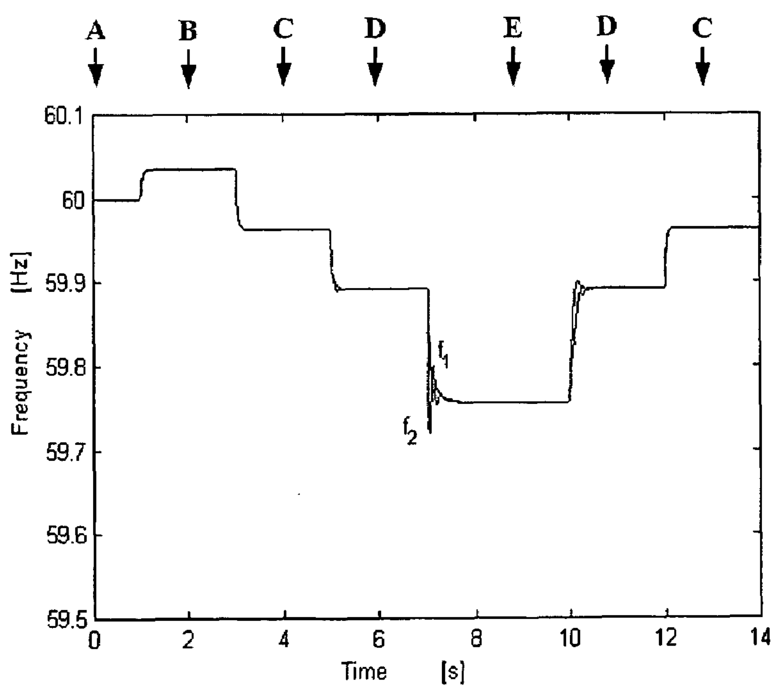

FIG. 25(b)

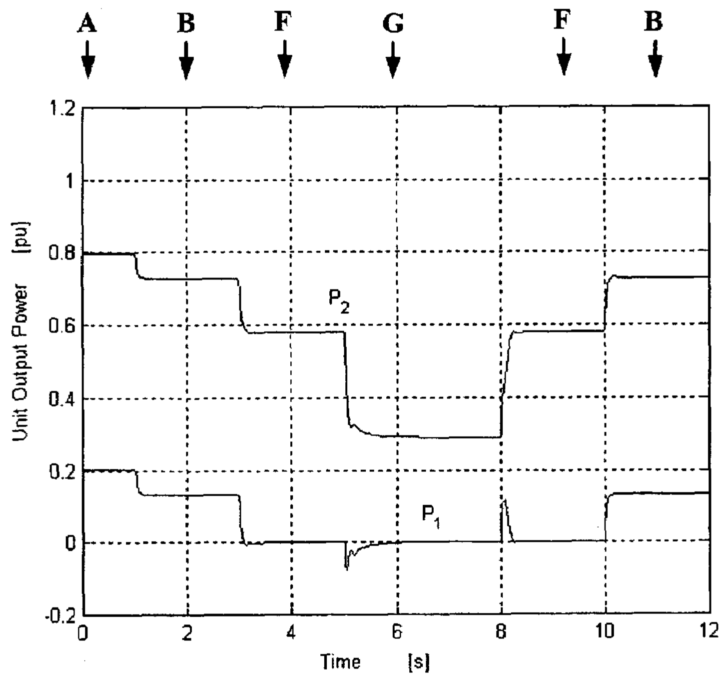

FIG. 26(a)

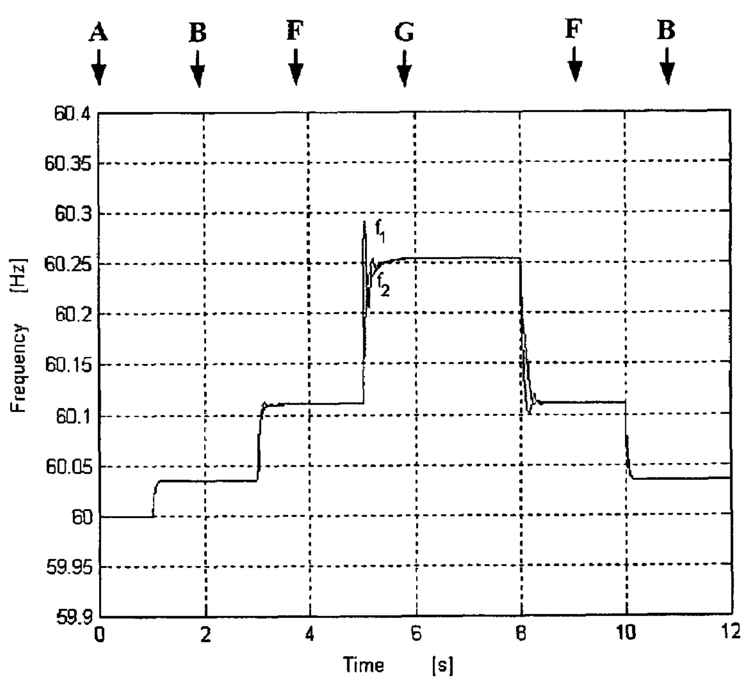

FIG. 26(b)

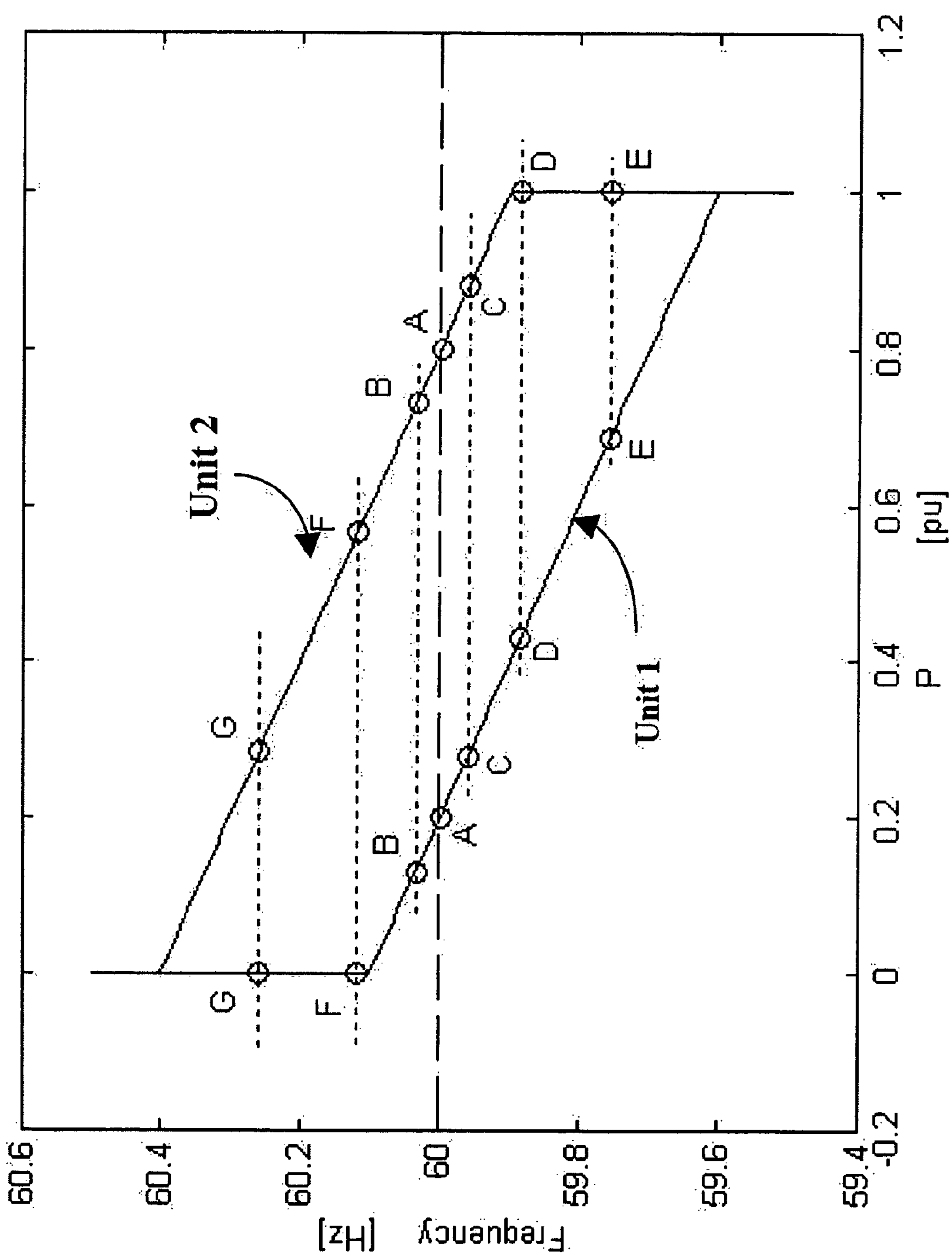
Unit 2
Unit 1
A
B
C
D
E
F
G
Frequency [Hz]
P [pu]
60.6
60.4
60.2
60
59.8
59.6
59.4
-0.2
0
0.2
0.4
0.6
0.8
1
1.2

FIG. 27

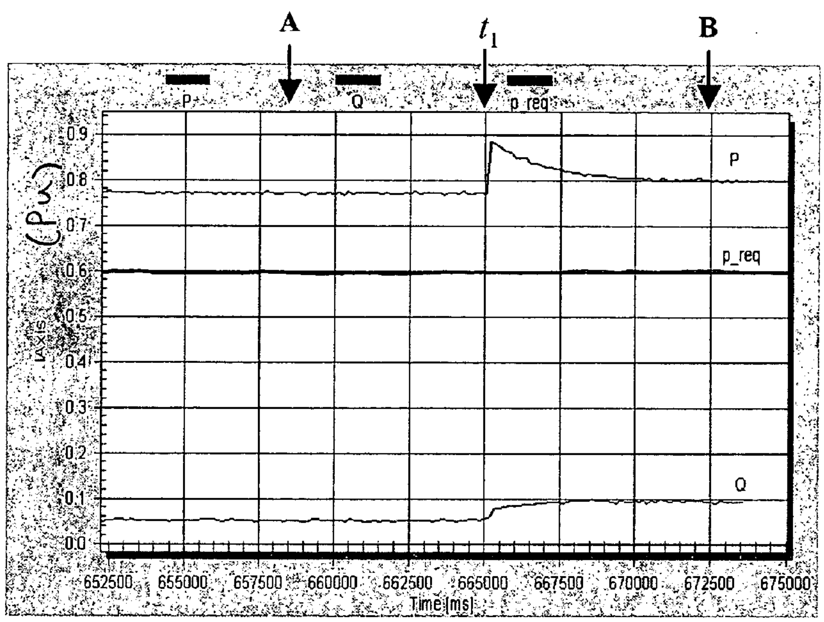

FIG. 28(a)

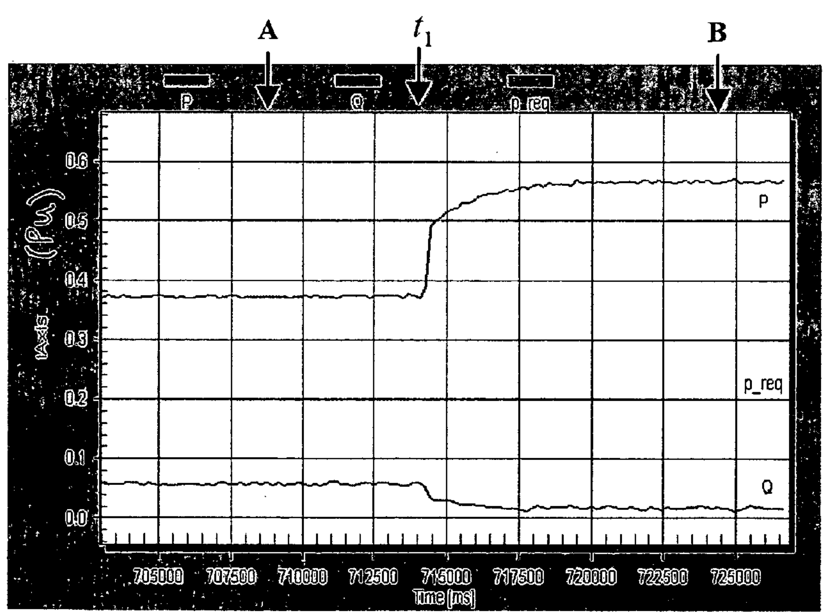

FIG. 28(b)

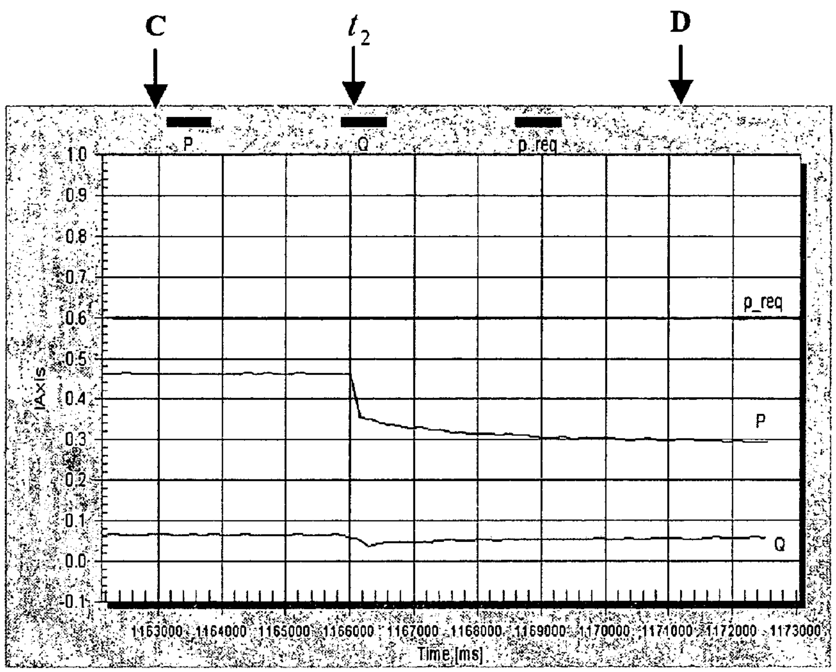

FIG. 29(a)

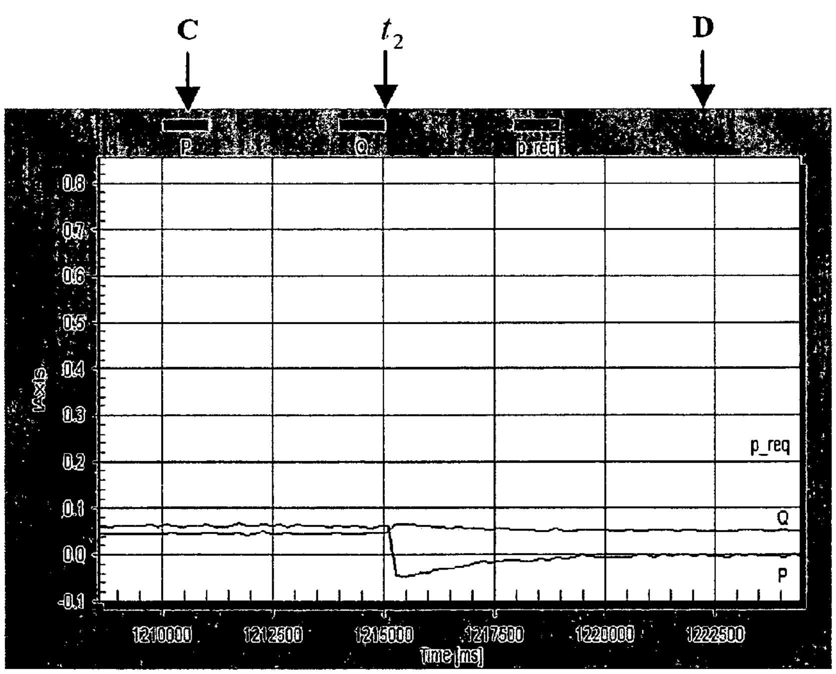

FIG. 29(b)

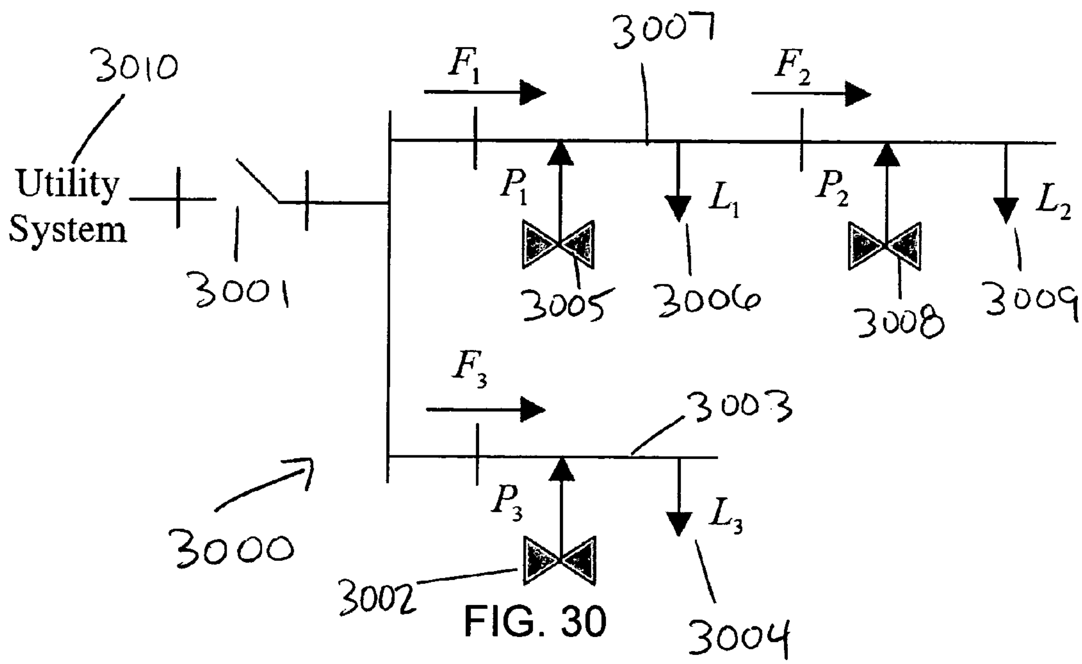
3010
Utility System
3001
3007
F_1
F_2
P_1
L_1
P_2
L_2
3005
3006
3008
3009
F_3
3003
P_3
L_3
3000
3002
3004

FIG. 30

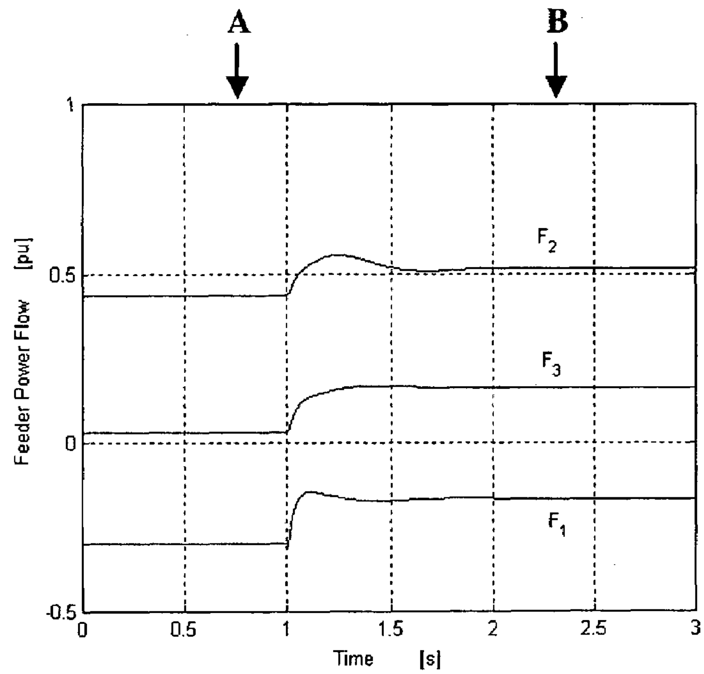

FIG. 31(a)

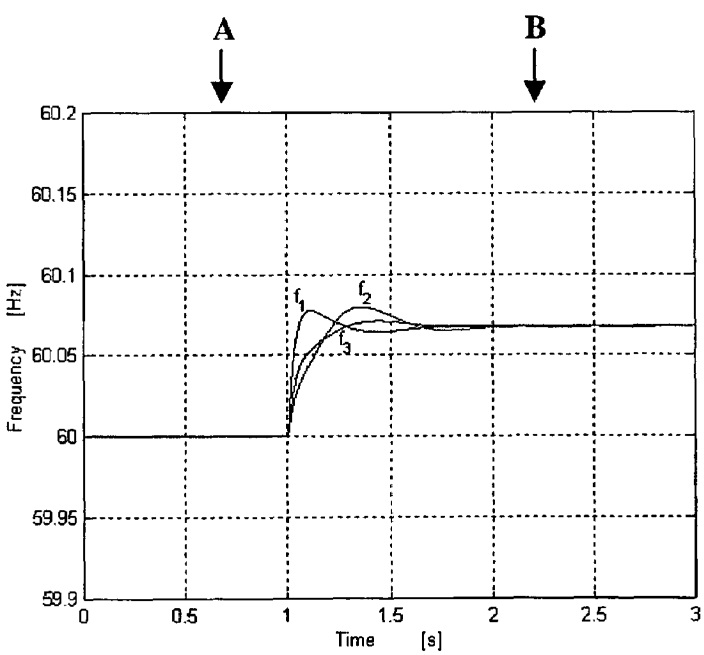

FIG. 31(b)

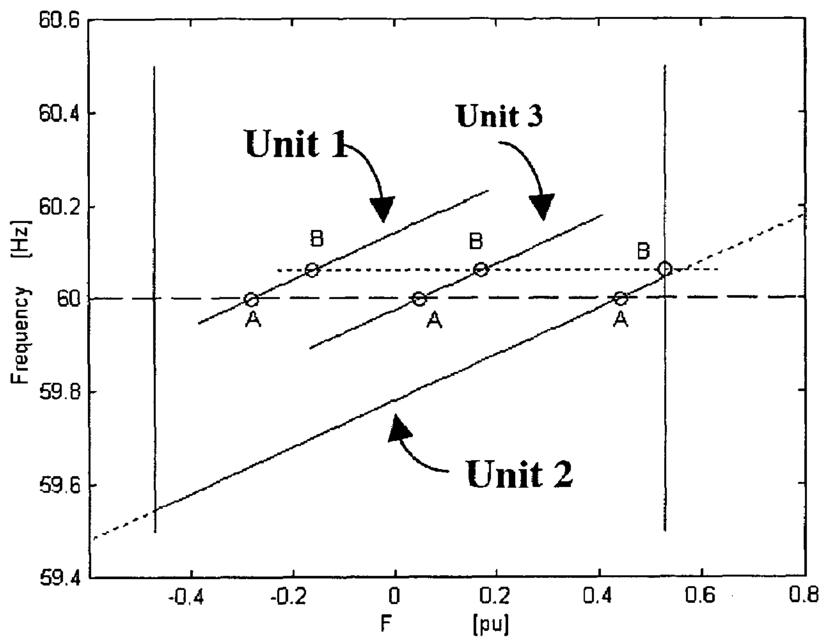

FIG. 32(a)

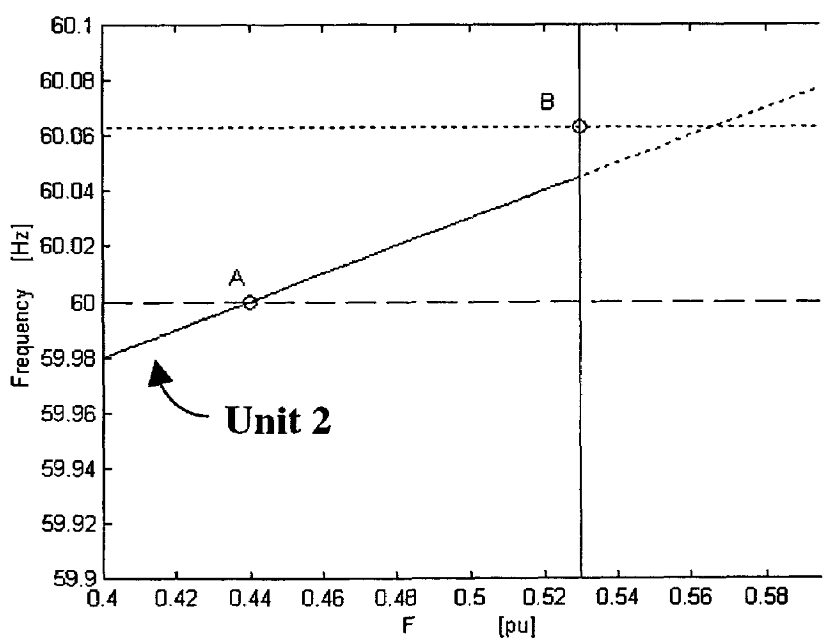

FIG. 32(b)

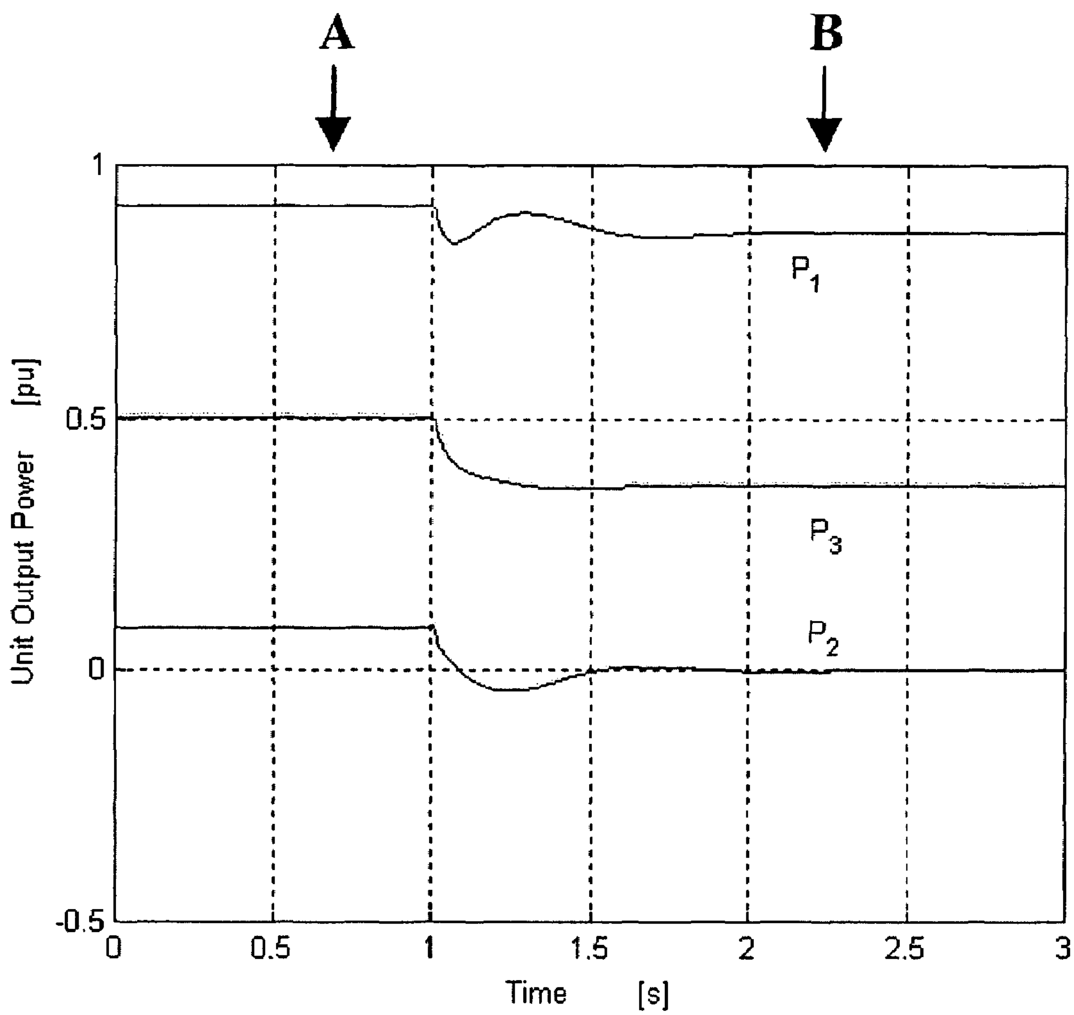

FIG. 33

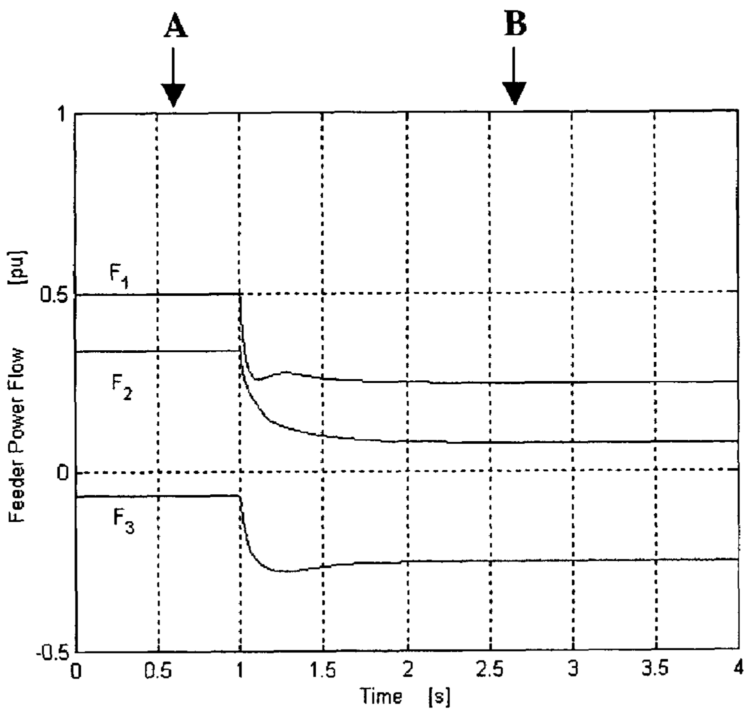

FIG. 34(a)

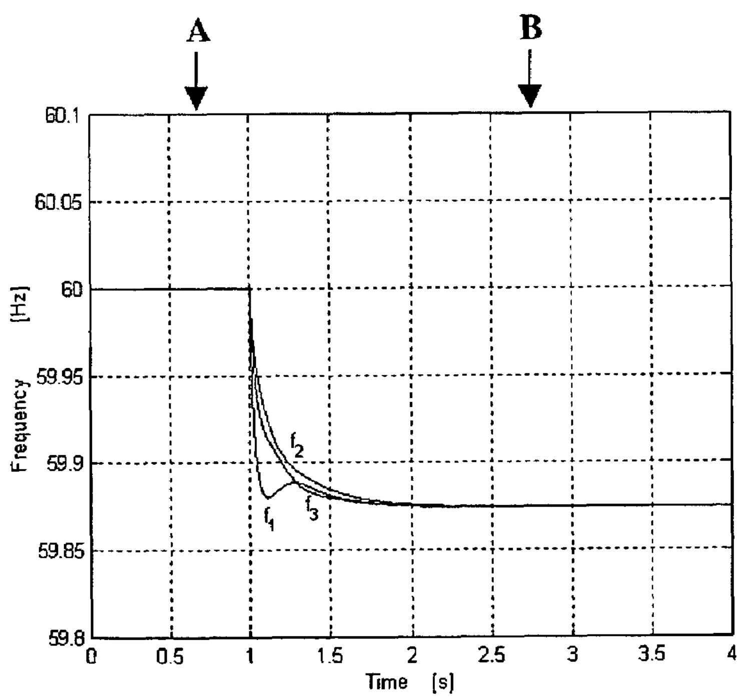

FIG.34(b)

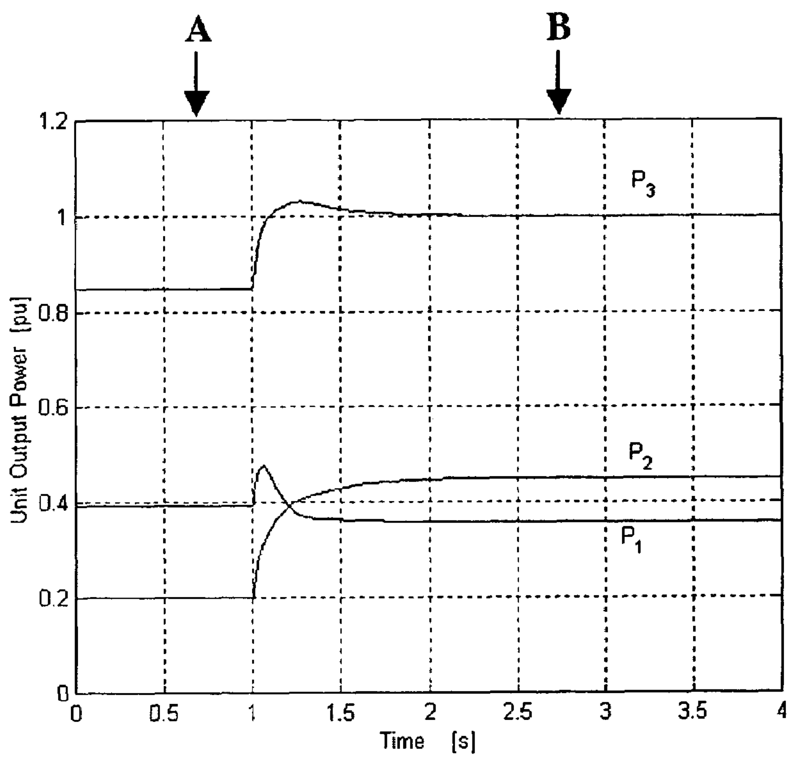
A
B
1.2
1
0.8
0.6
0.4
0.2
0
Unit Output Power [pu]
P3
P2
P1
0
0.5
1
1.5
2
2.5
3
3.5
4
Time [s]

FIG. 35

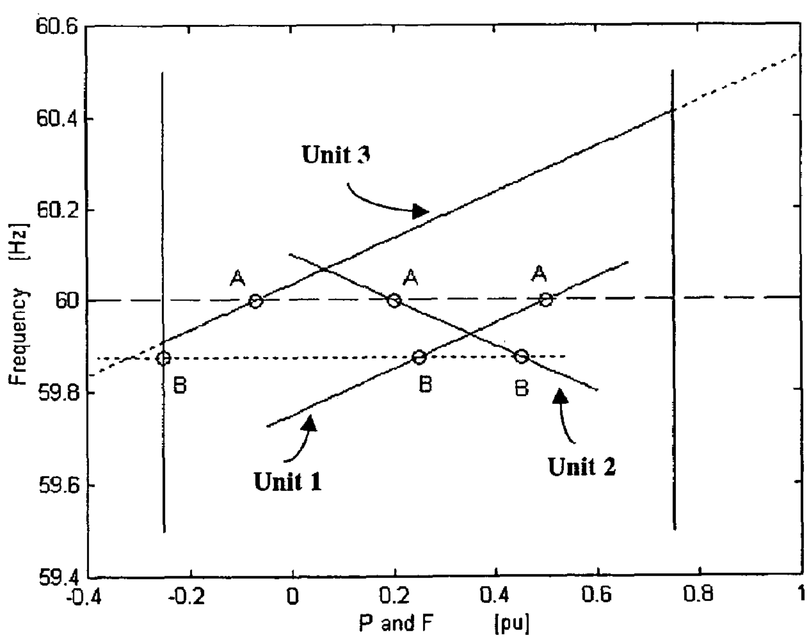
60.6
60.4
60.2
60
59.8
59.6
59.4
Frequency [Hz]
Unit 3
A
A
A
B
B
B
Unit 1
Unit 2
-0.4
-0.2
0
0.2
0.4
0.6
0.8
1
P and F [pu]

FIG. 36

CONTROL OF SMALL DISTRIBUTED ENERGY RESOURCES

REFERENCE TO GOVERNMENT RIGHTS

This invention was made with U.S. government support awarded by the following agencies:

DOE DE-AC03-76SF00098

NSF 0119230

The U.S. has certain rights in this invention.

FIELD OF THE INVENTION

The present invention relates generally to power systems and methods, including distributed energy resources (DER) systems and methods, and more particularly to devices and methods for controlling small distributed energy resources and/or associated loads.

BACKGROUND OF THE INVENTION

In the U.S. and around the world, the demand for electrical power continues to grow. At the same time, aging transmission and distribution systems remain subject to occasional failures. Massive failures covering wide geographical areas and affecting millions of people have occurred, even in the United States which has historically enjoyed a relatively robust electrical power system. These problems with the capacity and reliability of the public power grid have driven the development of distributed energy resources (DER), small independent power generation and storage systems which may be owned by, and located near, consumers of electrical power.

One motivating factor is that distributed energy resources can provide more reliable power in critical applications, as a backup to the primary electrical supply. For example, an interruption of power to a hospital can have life-threatening consequences. Similarly, when power to a factory is interrupted, the resulting losses, for example in productivity, wasted material in process that must be scrapped, and other costs to restart a production line, can be catastrophic. In situations like these, where the loss of electrical power can have serious consequences, the cost of implementing a distributed energy resource as a backup can be justified.

Reliability is not the only factor driving the development of distributed energy resources. Power from a distributed energy resource can, in some cases, be sold back to the main power grid. Geographically distributed sources of power, such as wind, solar, or hydroelectric power, may be too limited or intermittent to be used as the basis for a centralized power plant. By harnessing these types of geographically distributed sources using multiple distributed energy resources, these types of power sources can supplement or replace conventional power sources, such as fossil fuels, when the main power grid is available, and provide backup to their owners when the main power grid is unavailable.

In this context, distributed energy resources (DER) have emerged as a promising option to meet customers current and future demands for increasingly more reliable electric power. Power sources for DER systems, sometimes called "microsources," range in size and capacity from a few kilowatts up to 10 MW, they may include a variety of technologies, both supply-side and demand-side, and they are typically located where the energy is used.

Generally speaking, distributed energy resources can harness two broad categories of electrical power sources: DC sources, such as fuel cells, photovoltaic cells, and battery storage; and high-frequency AC sources, such as microturbines and wind turbines. Both types of sources are typically used to provide an intermediate DC voltage, that may be produced directly by DC sources, and produced indirectly from AC sources, for example by rectification. In both types of sources, the intermediate DC voltage is subsequently converted to AC voltage or current at the required frequency, magnitude, and phase angle for use. In most cases, the conversion from the intermediate DC voltage to the usable AC voltage is performed by a voltage inverter that can rapidly control the magnitude and phase of its output voltage.

Distributed energy resources are usually designed to operate in one of two modes: (1) "isolation" or "island" mode, isolated from the main grid, and (2) normal "grid" mode, connected to the main grid. For large utility generators, methods have been developed to allow conventional synchronous generators to join and to separate from the main electrical power grid smoothly and efficiently when needed. Because of fundamental differences between distributed energy resources, such as inverter based microsources or small synchronous generators, and centralized energy resources, these existing methods are not suitable to allow distributed energy resources to smoothly and efficiently transition between island mode and grid mode as the distributed energy resources join and separate from the main power grid.

For example, the fundamental frequency in an inverter is typically derived from an internal clock that does not change as the system is loaded. This arrangement is very different from that of synchronous generators typically used in centralized power systems, in which the inertia from spinning mass determines and maintains system frequency. Inverter-based microsources, by contrast, are effectively inertia-less, so alternative methods must be used to maintain system frequency in an inverter-based microsource.

Another difference between distributed energy resources and centralized energy resources relates to communication and coordination. A centralized electrical power utility is in a position to monitor and coordinate the production and distribution of power from multiple generators. In contrast, distributed energy resources may include independent producers of power who have limited awareness or communication with each other. Even if the independent producers of power are able to communicate with each other, there may not be any effective way to ensure that they cooperate.

Thus, there is a need for methods of controlling microsources in distributed energy resources to ensure that these resources can connect to or isolate from the utility grid in a rapid and seamless fashion, that reactive and active power can be independently controlled, and that voltage sag and system imbalances can be corrected. Further, there is a need for control of the microsources, and in particular the inverters used to supply power to the grid, based solely on information available locally at the inverter so that no communication or coordination between microsources is necessary. Yet further, there is a need for a local controller at the microsource to enable "plug and play" operation of the microsource. In other words, there is a need to add microsources to a distributed energy resource system without changes to the control and protection of units that are already part of the system.

SUMMARY OF THE INVENTION

An exemplary embodiment of the invention relates to a method of controlling the output inverter of a microsource in a distributed energy resource system, using a unit power controller that reduces the operating frequency of the inverter to increase its unit output power. In a preferred embodiment of the invention, the inverter reaches maximum output power and minimum operating frequency at the same time, and it includes a voltage controller implementing a voltage vs. reactive current droop. Other aspects of this embodiment relate to an inverter that implements such methods, and a microsource containing such an inverter. These methods can be extended to control inverters in a plurality of microsources, where the rate of change of frequency vs. power for each microsource depends on its power set point.

Another embodiment of the invention relates to a method of controlling the output inverter of a microsource in a distributed energy resource system, using a unit power controller that reduces the operating frequency of the inverter to increase its unit output power, with the rate of change of frequency vs. power having at least two different values over the operating range of the inverter. In a preferred embodiment of this method, the inverter reaches maximum output power and minimum operating frequency at the same time, and includes a voltage controller that implements a voltage vs. reactive current droop. In some embodiments, the rate of change of power vs. frequency may be zero when the inverter reaches its minimum or maximum power limits, and the rate of change of frequency vs. power may be zero when the inverter reaches its frequency limits. Other aspects of this embodiment relate to an inverter that implements such methods, and a microsource containing such an inverter. This embodiment also can be extended to control inverters in a plurality of microsources, where the rate of change of frequency vs. power for each microsource depends on its power set point.

Another embodiment of the invention relates to a method of controlling the output inverters of a plurality of microsources in a distributed energy resource system, each using a unit power controller that reduces the operating frequency of the inverter to increase its unit output power, with the rate of change of frequency vs. power being the same for each microsource over the operating range of its inverter. In preferred embodiments of this method, each inverter uses a voltage controller that includes a voltage vs. reactive current droop. In some embodiments, the rate of change of power vs. frequency may be zero when the inverter reaches its minimum or maximum power limits, and the rate of change of frequency vs. power may be zero when the inverter reaches its frequency limits. Other aspects of this embodiment relate to an inverter that implements such methods, and a microsource containing such an inverter.

Another embodiment of the invention relates to a method of controlling the output inverter of a microsource in a distributed energy resource system, using a zone power controller that reduces the operating frequency of the inverter to reduce its zone power flow. In a preferred embodiment of the invention, the inverter includes a voltage controller implementing a voltage vs. reactive current droop. Other aspects of this embodiment relate to an inverter that implements such methods, and a microsource containing such an inverter. These methods can be extended to control inverters in a plurality of microsources, where the microsources may be arranged in one or more zones.

Other principal features and advantages of the invention will become apparent to those skilled in the art upon review of the following drawings, the detailed description, and the appended claims.

BRIEF DESCRIPTION OF THE DRAWINGS

FIG. **1** is a diagram of an exemplary distributed energy resource system;

FIG. **2** is a diagram of an exemplary microsource that can be used in a distributed energy resource system such as that of FIG. **1**;

FIG. **3** is a diagram of an inverter control system that can be used with a microsource such as that of FIG. **2**, in a distributed energy resource system such as that of FIG. **1**;

FIG. **4** is a diagram of the state variables in an exemplary distributed energy resource system, such as that of FIG. **1**, that includes an exemplary microsource, such as that of FIG. **2**;

FIG. **5** is a diagram of a voltage controller in accordance with an exemplary embodiment of the invention for use in a microsource system;

FIG. **6** is a graph of an exemplary voltage droop regulation characteristic for a voltage controller in a single microsource;

FIG. **7** is a diagram of an exemplary industrial plant including microsource systems in accordance with the invention;

FIGS. **8**(*a*) and **8**(*b*) are graphs of predicted real power and reactive power, respectively, obtained using a computer simulation of the circuit of FIG. **7** as the exemplary microsources of FIG. **7** are brought online in grid-connected mode;

FIGS. **9**(*a*) and **9**(*b*) are graphs of predicted regulated voltage on bus **738** and bus **739**, respectively, in the exemplary industrial plant of FIG. **7**, obtained using a computer simulation of the circuit of FIG. **7** as the exemplary microsources of FIG. **7** are brought online in grid-connected mode;

FIGS. **10**(*a*), **10**(*b*), and **10**(*c*) are graphs of predicted regulated voltages on bus **738**, bus **739**, and the 13.8 kV feeder **710**, respectively, in the exemplary industrial plant of FIG. **7**, obtained using a computer simulation of the circuit of FIG. **7** during a transfer to island mode;

FIGS. **11**(*a*) and **11**(*b*) are graphs of predicted real power and reactive power, respectively, of the microsources in the exemplary industrial plant of FIG. **7**, obtained using a computer simulation of the circuit of FIG. **7** during a transfer to island mode;

FIG. **12** is a diagram of a unit power controller in accordance with an exemplary embodiment of the invention for use in a microsource system;

FIG. **13** is a diagram of a microgrid that includes a microsource implementing a unit power control scheme in accordance with an exemplary embodiment of the invention;

FIG. **14** is a graph depicting the relationship between steady state unit power vs. frequency (P-ω) in a unit power control scheme having a variable slope, for two exemplary microsources having different power set points;

FIG. **15** is a graph depicting the relationship between steady state unit power vs. frequency (P-ω) in a unit power control scheme having variable slope with power and frequency limits, for two exemplary microsources having different power set points;

FIG. **16** is a graph depicting the relationship between steady state unit power vs. frequency (P-ω) in a unit power control scheme having a fixed slope, for two exemplary microsources having different power set points;

FIG. **17** is a graph depicting the relationship between steady state unit power vs. frequency (P-ω) in a unit power control scheme having a fixed minimum slope, for two exemplary microsources having different power set points;

FIG. **18** is a diagram of a unit power controller with upper and lower power limits in accordance with an exemplary embodiment of the invention;

FIG. **19** is a diagram of a microsource implementing a zone power control scheme in accordance with an exemplary embodiment of the invention;

FIG. **20** is a graph depicting the relationship between steady state zone power vs. frequency (P-ω) in a zone power control scheme having a fixed minimum slope, for two exemplary microsources having different power set points;

FIG. **21** is a diagram of an exemplary system with two microsources installed in a single zone;

FIG. **22** is a diagram of an exemplary system with two microsources installed in two zones;

FIG. **23** is a graph depicting the relationship between steady state zone power vs. frequency (P-ω) in a zone power control scheme having fixed minimum slope and unit power limits, for two exemplary microsources having different power set points;

FIG. **24** is a diagram of a zone power controller with upper and lower unit power limits in accordance with an exemplary embodiment of the invention;

FIGS. **25**(*a*) and **25**(*b*) are graphs of predicted output power and instantaneous frequency, respectively, from the microsources in the system of FIG. **21**, obtained using a computer simulation of unit power control during a transfer to island mode with a first series of loads added and removed;

FIGS. **26**(*a*) and **26**(*b*) are graphs of predicted output power and instantaneous frequency, respectively, from the microsources in the exemplary system of FIG. **21**, obtained using a computer simulation of unit power control during a transfer to island mode with a second series of loads added and removed;

FIG. **27** is a graph depicting the relationship between steady state unit power vs. frequency (P-ω) in a unit power control scheme according to the invention applied to the system of FIG. **21**, showing the steady state operation points (A)-(G) of FIGS. **25-26**;

FIGS. **28**(*a*) and **28**(*b*) are graphs of predicted real power (P) and reactive power (Q) from the microsources **2102** and **2105**, respectively, in the exemplary system of FIG. **21**, obtained using a hardware simulation of unit power control with a load added when the system is in steady state island mode;

FIGS. **29**(*a*) and **29**(*b*) are graphs of predicted real power (P) and reactive power (Q) from the microsources unit **1** and unit **2**, respectively, in the exemplary system of FIG. **21**, obtained using a hardware simulation of unit power control with a load removed when the system is in steady state island mode;

FIG. **30** is an exemplary system having two zones, an upper zone with two microsource units, and a lower zone with one microsource unit;

FIGS. **31**(*a*) and **31**(*b*) are graphs of predicted zone power flow and instantaneous frequency, respectively, from the microsources in the exemplary system of FIG. **30**, obtained using a computer simulation of zone power control during a transfer to island mode;

FIG. **32**(*a*) is a graph depicting the relationship between steady state frequency vs. zone power flow in a zone power control scheme according to the invention applied to the system of FIG. **30**, showing the steady state operation points (A)-(B) of FIGS. **31**(*a*)-**31**(*b*), and FIG. **32**(*b*) is a magnification of the relationship of FIG. **32**(*a*) for unit **2**;

FIG. **33** is a graph of the predicted unit real power flow from the microsources in the exemplary system of FIG. **30**, obtained using a computer simulation of zone power control during a transfer to island mode;

FIGS. **34**(*a*) and **34**(*b*) are graphs of predicted zone power flow and instantaneous frequency, respectively, from the microsources in the exemplary system of FIG. **30**, obtained using a computer simulation of a mix of zone and unit power control during a transfer to island mode;

FIG. **35** is a graph of the predicted unit real power flow from the microsources in the exemplary system of FIG. **30**, obtained using a computer simulation of a mix of zone and unit power control during a transfer to island mode;

FIG. **36** is a graph depicting the relationship between steady state frequency vs. zone and unit power flow in a mixed zone and unit power control scheme applied to the system of FIG. **30**, showing the steady state operation points (A)-(B) of FIGS. **34**(*a*)-**34**(*b*), and FIG. **35**.

DETAILED DESCRIPTION OF THE PREFERRED EMBODIMENTS

Referring to the figures, FIG. **1** is a diagram of an exemplary distributed energy resource system. Such an exemplary system is described, for example, in U.S. Patent Application Publication No. US 2004/0051387, the contents of which are incorporated by reference. In the event of any conflict between the disclosure of the present application and the disclosure of U.S. Patent Application Publication No. US 2004/0051387, the disclosure of the present application controls.

The present invention relates to a system for and method of control of small distributed energy resources. This control can be implemented by changing the phase of the output from the microsource as a function of time, to vary the instantaneous frequency and power of that output.

The invention relates more particularly to novel control schemes for controlling the instantaneous frequency and power from one or more microsources in ways that tend to ensure that the microsources stay within their normal operating ranges and otherwise operate effectively. The novel control schemes focus on what needs to be done in response to events such as islanding or new loads to transition smoothly between stable steady state frequency and power operating points.

The scope of the invention is not limited to any particular hardware circuitry that can be used to implement the control schemes of the present invention. A variety of hardware circuitry can be used to implement the control schemes of the present invention. In some embodiments, hardwired circuitry may be used in place of, or in combination with, software instructions to implement the functions described. Thus, the embodiments described herein are not limited to any specific combination of hardware circuitry and software, nor to any particular source for the instructions executed by a computerized control system.

In the following description, for purposes of explanation, numerous specific details are set forth to provide a thorough understanding of exemplary embodiments of the invention. It will be evident, however, to one skilled in the art that the invention may be practiced without these specific details. In other instances, structures and devices are shown in block diagram form to facilitate description of the exemplary embodiments.

The exemplary control schemes of the present invention are directed to ensuring that: (1) new generators can be added to the system without modification of existing equipment; (2) a collection of sources and loads can connect to or isolate from the utility grid in a rapid and seamless fashion; (3) each inverter can respond effectively to load changes without requiring data from other sources; and (4) voltage sag and system imbalances can be corrected.

The system and method for control of small distributed energy resources can be implemented in a wide variety of different ways. Various embodiments may include, for example, DC sources or AC sources. The invention is not limited to a particular embodiment, but extends to various modifications, combinations, and permutations within the scope of the appended claims.

FIG. **1** is a diagram of an exemplary distributed energy resource system **100** including a utility supply **110** connected to one or more feeder lines **115** that interconnect microsource systems **120**, **130**, **140**, and **150** and one or more loads **160**. Each microsource system **120**, **130**, **140**, and **150** preferably includes a microsource controller **300**. The feeder line **115**, the interconnected microsource systems **120**, **130**, **140**, and **150**, and the one or more loads **160** can form a microgrid **117**. In a distributed energy resource (DER) system, the utility supply **110** can connect the microgrid **117** to other similar microgrids distributed throughout the DER system.

The microsource systems **120**, **130**, **140**, and **150** can include exemplary microsource power sources, power storage, and power controllers. The power source can be, for example, a fuel cell, hydroelectric generator, photovoltaic array, windmill, or microturbine. The power storage, if present, can be, for example, a battery or flywheel. The controller can, for example, control an inverter that determines the flow of power out of the microsource.

The feeder line **115** may include one or more interface switches **118**. The interface switch **118**, if used, can be positioned between the feeder line **115** and the main utility supply **110** so that the microgrid **117**, comprised of the feeder line **115**, the interconnected microsource systems **120**, **130**, **140**, and **150**, and the one or more loads **160**, can be isolated from the utility supply **110**. When the microgrid **117** is isolated from the utility supply **110**, the microgrid **117** is said to be operating in “island mode.” Similarly, when the microgrid **117** is connected to the utility supply **110**, the microgrid **117** is said to be operating in “grid mode.”

The interface switch **118**, if used, can be positioned in other places, for example between portions of the microgrid **117**, or between a particular microsource and the feeder line **115**, thereby allowing a portion of the microgrid or a particular microsource to be operated in either island mode or grid mode.

When a microsource or microgrid operates in island mode, load tracking problems can arise because typical power sources in microsources, such as microturbines or fuel cells, tend to respond slowly, with time constants ranging from 10 to 200 seconds, and these types or power sources are generally inertialess. Conventional utility power systems store energy in the inertia of the spinning mass of a generator. When a new load comes online, the initial energy balance can be met by the system’s inertia, which results in a slight reduction in system frequency. Because power sources in microsources are inertialess, a microsource will often include at least some power storage to ensure initial energy balance when loads are added during island mode.

Power storage for a microsource during island operation can come in several forms: batteries or super-capacitors on the DC bus; direct connection of AC storage devices (batteries, flywheels etc.); or use of local traditional generation that has inertia along with the microsource. Note that if a microsource never operates in island mode, the energy imbalance can be met by the utility supply, so power storage may not be necessary in that case.

In at least one of the exemplary embodiments, the microsource control methods described below can be used to control inverter interfaces found in fuel cells, photovoltaic panels, micro turbines, variable internal combustion engines, wind turbines, and storage technologies. Advantageously, communication among microsources is unnecessary for basic system control. Each inverter responds effectively to load changes without requiring data from other sources or locations.

FIG. **2** is a diagram of an exemplary microsource **200** that can be used in a distributed energy resource system such as that of FIG. **1**. The microsource **200** can include a prime mover **210**, a DC interface **220** and a voltage source inverter **230**. The microsource **200** may also include power storage **215**, for example a battery, although this is not required. The prime mover **210** can be, for example, a fuel cell, micro turbine, PV, or wind turbine. The controller for the microsource **200** is not shown in FIG. **2**.

The microsource **200** couples, for example using an inductor **240**, to a power system **250** that provides a system voltage $\overline{E}$ at the connection point between the microsource **200** and the power system **250**. The inverter **230** controls both the magnitude and phase of its output voltage $\overline{V}$. The vector relationship between the inverter output voltage $\overline{V}$ and the system voltage $\overline{E}$ along with the reactance X of the inductor **240** determines the flow of real and reactive power (P & Q) between the microsource **200** and the system **250**.

P & Q magnitudes are determined as shown in the equations (1), (2), and (3) below. When the power angle δ_p (the difference in phase between $\overline{E}$ and $\overline{V}$) is small, $\sin(\delta_p)$ is approximately δ_p and $\cos(\delta_p)$ is approximately 1, as can be seen from a power series expansion of sin(x) and cos(x). So, when δ_p is small, P is predominantly dependent on the power angle δ_p, and Q is dependent on the magnitude of the output voltage $\overline{V}$ of the inverter **230**. These relationships constitute a basic feedback loop for the control of output real power P and reactive power Q through regulation of the power angle δ_p and/or the inverter output voltage $\overline{V}$ in response to measurements of system voltage $\overline{E}$.

$$P = \frac{3}{2}\frac{VE}{X}\sin\delta_p \qquad \text{[Eq. 1]}$$

$$Q = \frac{3}{2}\frac{V}{X}(V - E\cos\delta_p) \qquad \text{[Eq. 2]}$$

$$\delta_p = \delta_V - \delta_E \qquad \text{[Eq. 3]}$$

In a system that includes a plurality of microsources such as the system **100** of FIG. **1**, communication between microsources may be difficult or impossible especially when microsources come and go independently. Further, even if communication between microsources were possible, there may be no way to ensure cooperation between microsources owned or operated by independent entities. Advantageously, the control schemes of the present invention do not require any communication or coordination between microsources. Instead, the control schemes of the present invention depend only on measurements that are available locally, such as $\overline{V}$ and $\overline{E}$ in FIG. **2** or current flows, for example through the inductor **240**.

FIG. **3** is a diagram of a controller **300** that can be used with a microsource such as that of FIG. **2**, for example to control an inverter that regulates power flow from the microsource in a distributed energy resource system such as that of FIG. **1**. The controller **300** can include a real and reactive power (P&Q) calculator **310**, a flux vector or phasor calculator **320**, a voltage controller **330**, a power controller **340**, and an inverter **350** although it is not necessary that the controller **300** include all of these components. The controller **300** preferably has a fast response time on the order of a few milliseconds. The inverter **350** can be, for example, a pulse width modulation (PWM) inverter.

Exemplary inputs to the controller **300** can include three set points and three measured states. Set points can include E_0: the voltage set point at the output of the inverter; P_0: the power set point of power flow from the microsource; and ω_o: the operating frequency set point of the inverter. Measured state variables can include $\overline{E}$: the system voltage at the connection point; $\overline{I}_{inductor}$: the time varying current injected by the microsource; and $\overline{I}_{feeder}$: the time varying current in the feeder. $\overline{I}_{inductor}$ would typically be used in a unit power control scheme, and $\overline{I}_{feeder}$ would typically be used in a zone power control scheme. All of these measured state variables can be obtained from instantaneous voltage or current measurements that can be made locally.

The controller **300** can supply one or more output variables to control the inverter **350**. For example, the voltage controller **330** can supply the magnitude of the inverter output voltage flux $|\Psi_v|$ or the magnitude of the inverter output voltage $|V|$. The power controller can supply the phase angle of the inverter output voltage δ_v.

The P & Q calculator **310** can have three inputs: $\overline{E}$, $\overline{I}_{inductor}$, and $\overline{I}_{feeder}$ which are used to calculate the real power P and the reactive power Q. The P & Q calculator **310** can calculate either the real power P being injected by the microsource using the inductor current, $\overline{I}_{inductor}$, or the real power P flowing through the feeder line using the feeder current, $\overline{I}_{feeder}$, depending on whether a unit power scheme or a zone power scheme is being implemented. The reactive power is the Q being injected by the microsource. The real power P can be supplied to the power controller **340**, and the reactive power Q can be supplied to the voltage controller **330**.

The flux vector or phasor calculator **320** can calculate the instantaneous magnitude $|E|$ and phase δ_e of the system voltage $\overline{E}$ at the point where the microsource is connected. Note that the phase δ_e of the system voltage $\overline{E}$ is not required by either the voltage controller **330** or the power controller **340** in the controller **300**. The flux vector or phasor calculator **320** can also calculate the time-integral of the system voltage $\overline{E}$, referred to as the system voltage flux vector $\overline{\Psi}_e$:

$$\Psi_E(t)=\Psi_E(t_O)+\int_o E d\tau \quad \text{[Eq. 4]}$$

The system voltage flux vector Ψ_e can be calculated, for example, by transforming the three phase input phase voltages, E, to the stationary d-q reference frame by means of [Eq. 5], where e_{ds} (t) is the component of system voltage along a d axis of the d-q reference frame at time t, $_{qs}$ (t) is the component of system voltage along a q axis of the d-q reference frame at time t, e_a (t) is first phase voltage of the three phase input voltage at time t, e_c (t) is a second phase voltage of the three phase input voltage at time t, and e_c (t) is a third phase voltage of the three phase input voltage at time t.

$$e_{ds}(t) = \frac{e_c(t) - e_b(t)}{\sqrt{3}} \quad \text{[Eq. 5]}$$

$$e_{qs}(t) = \left(\frac{2}{3}\right)\left(e_a(t) - \frac{1}{2}e_b(t) - \frac{1}{2}e_c(t)\right)$$

These voltages $e_{ds}(t)$ and $e_{qs}(t)$ can be integrated to yield the d-q components of the system voltage flux vector in rectangular coordinates:

$$\Psi_{ed}=\int_{-\infty}^{t} e_{ds}(\tau)d\tau$$

$$\Psi_{eq}=\int_{\infty}^{t} e_{qs}(\tau)d\tau \quad \text{[Eq. 6]}$$

The system voltage flux vector in rectangular coordinates can then be transformed to polar quantities $|\Psi_e|$ and δ_e:

$$|\Psi_e| = \sqrt{\Psi_{ed}^2 + \Psi_{eq}^2} \quad \text{[Eq. 7]}$$

$$\delta_e = -\tan^{-1}\left(\frac{\Psi_{ed}}{\Psi_{eq}}\right)$$

The operation of the voltage controller **330** is explained further below in reference to FIGS. **4-6**, and the operation of the power controller **340** is explained further below in reference to FIGS. **12-23**.

FIG. **4** is a diagram of the state variables in a distributed energy resource system **400** that includes an exemplary microsource **420**. The distributed energy resource system **400** includes a utility supply **410** providing a feeder current $\overline{I}_{feeder}$ through a feeder line **415**, and a microsource **420** providing an inductor current $\overline{I}_{inductor}$ through an inductor **430**. A system voltage $\overline{E}$ can be measured at the external side **425** of the inductor **430** that connects to the feeder line **415**. These state variables, $\overline{E}$, $\overline{I}_{feeder}$, and $\overline{I}_{inductor}$ are used by the P & Q calculator **310** described with reference to FIG. **3** to calculate real power P and reactive power Q, with $\overline{I}_{feeder}$ typically used in a zone power control scheme and $\overline{I}_{inductor}$ typically used in a unit power control scheme.

A microsource output voltage $\overline{V}$ can be measured at the internal side **435** of the inductor **430** that connects to the microsource output, for example an inverter output. The system **400** may include one or more loads **450**. The system **400** may also include a switch **440** that can be opened to isolate the microsource **420** and loads **450** from the utility supply **410**, and that can be closed to connect the microsource **420** and loads **450** to the utility supply **410**.

Conventionally, integration of large numbers of microsources into a system is not possible with basic P-Q controls; voltage regulation is necessary for local reliability and stability. Without local voltage regulation, systems with high penetrations of microsources can experience voltage and or reactive power oscillations. Voltage regulation can ensure that there are no large circulating reactive currents between sources.

FIG. **5** is a diagram of an exemplary voltage controller **500** for use in a microsource system, which can be, for example, the voltage controller **330** described with reference to FIG. **3**. There are three inputs to the exemplary voltage controller **500**. One input is E_0, the inverter output voltage set point. Another input is Q, the reactive power being injected by the microsource. A third input is either the magnitude of the system voltage flux $|\Psi_e|$ or the magnitude of the measured system voltage $|E|$. The voltage controller **500** preferably includes voltage vs. reactive current droop with slope M_V (explained further below).

The gain K depends on whether the magnitude of the system voltage flux $|\Psi_e|$ or the magnitude of the measured system voltage $|E|$ is used in the calculation. In an exemplary embodiment, K=1 if the measured system voltage $|E|$ is used in the calculation, and $K=1/\omega_o$ if the magnitude of the system voltage flux $|\Psi_e|$ is used.

In the exemplary voltage controller **500**, the inverter output voltage set point E_0 is added to the product of the voltage droop slope M_v and the reactive power Q using a summer **510**. The resulting total is multiplied by the gain K. The resulting product is added to either the magnitude of the measured system voltage flux $|\Psi_e|$ or the magnitude of the measured system voltage $|E|$ using a summer **520**. The resulting difference between the drooped voltage set point and the measured system voltage is voltage error is input to a PI (proportional plus integral) controller, which can supply either the magnitude of the inverter output voltage flux $|\Psi_v|$ or the magnitude of the inverter output voltage |V| to an inverter, such as the inverter **350** of FIG. **3**.

The voltage regulation issues for microsources are similar to those involved in control of large synchronous generators. However, the impedance between generators in the power grid is usually large enough to greatly reduce the possibility of circulating currents. In contrast, the impedance between microsources in a distributed energy resource system may be relatively small, so small errors in voltage set points can give rise to relatively large circulating reactive currents which can exceed the ratings of the microsources.

For the foregoing reasons, the voltage controller **500** for a microsource in a distributed energy resource system preferably includes voltage vs. reactive current droop. FIG. **6** is a graph of an exemplary voltage droop regulation characteristic for a voltage controller on a microsource, such as the controller shown in FIG. **5**. When the microsource generates capacitive reactive power, −Q, the voltage set point is lowered as defined by the slope. When the microsource generates inductive reactive power, Q, the voltage set point is increased.

FIG. **7** is a diagram of an exemplary industrial plant **700** including microsource systems in accordance with the invention. The exemplary industrial plant **700** can have high motor loads M**5**, M**8**, M**7**, and M**9** that comprise, for example, 1.6 MW of motor load with motors ranging from 50 to 150 hp each, to illustrate the dynamics of the microsource controls described with reference to FIGS. **1**-**6**. In this example, a 120 kV utility supply **705** provides power to the plant **700** through a long 13.8 kV feeder line **710** that includes overhead lines **715** and underground cables **720**.

The feeder line **710** terminates in a switch **725** that connects the feeder line **710** to the power bus **730**. The switch **725** can be opened to operate the plant **700** in island mode, disconnecting the entire plant **700** from the feeder line **710** and utility supply **705**. The switch **725** can also be closed to operate the plant **700** in grid mode, with the plant **700** connected to the feeder line **710** and utility supply **705**. The power bus **730** supplies power to three feeders, a first feeder **735** at 480V, a second feeder **740** at 480V, and a third feeder **745** at 2.4kV. The third feeder **745** is connected to the power bus **730** by a second switch **732** that allows the third feeder **745** and its load M**7** to be disconnected from the remainder of the plant **700**.

In the exemplary plant **700**, the loads on the 480V feeders **735** and **740** are presumed to be critical and must continue to be served if utility power is lost. The first 480V feeder **735** supplies power to bus **737**, which serves load M**5** and bus **738**. Bus **738** includes load M**8**, presumed to be an induction machine, capacitive voltage support **750**, and a first microsource **755**. The second 480V feeder **740** supplies power to bus **739**, which serves load M**9**, presumed to be an induction machine, capacitive voltage support **760**, and a second microsource **765**.

The exemplary microsources **755** and **765** provide both power injection and local voltage support, and are each assumed to be rated at 600 KVA maximum power. When the microsources **755** and **765** are offline and not generating power, calculations show that the voltages of buses **738** and **739** are 0.933 and 0.941 per unit (pu, on 480-V base), respectively, and total losses are 70 kW. The microsource power injection is approximately one half the total power. With microsources **755** and **765** operating, the voltages on buses **738** and **739** are regulated at 1 pu. Because the power from the microsources is generated locally, the total losses drop to 6 kW, a reduction of 64 kW due to reduced transmission losses through the long 13.8 kV feeder line **710**.

FIGS. **8**(*a*) and **8**(*b*) are graphs of predicted real power and reactive power, respectively, on bus **738** (P**8**, Q**8**) and bus **739** (P**9**, Q**9**) in the exemplary industrial plant **700**. FIGS. **9**(*a*) and **9**(*b*) are graphs of predicted regulated voltage on bus **738** and bus **739**, respectively, in the exemplary industrial plant **700**. These results were obtained using a computer simulation of the circuit of FIG. **7** as the exemplary microsources **755** and **765** are brought online in grid-connected mode (with switches **725** and **732** both closed).

FIGS. **8**(*a*) and **8**(*b*) show the active and reactive power injections at the buses where units are located. In the initial state at t=0, microsources **755** and **765** are offline, so FIGS. **8**(*a*) and **8**(*b*) show zero real and reactive power injection. Similarly, FIGS. **9**(*a*) and **9**(*b*) show reduced voltages on buses **738** and **739** at t=0.

At t=1, microsource **755** on bus **738** is brought online with a power setting of 446 kW and local voltage control. Note the voltage correction shown as a slight rise at t=1 in graph **930** of FIG. **9**(*a*).

At t=3, microsource **765** on bus **739** is brought online with a power set point of 360 kW and local voltage control, which is reflected in a slight rise in voltage at t=3 in graph **940** of FIG. **9**(*b*). Note that FIG. **8**(*b*) shows the Q injection from microsource **755** (P**8**, Q**8**) to maintain local voltage magnitude at bus **738** drops at t=3 as the second microsource **765** (P**9**, Q**9**) is brought online.

This example can also be used to simulate island operation with power sharing through droop. In the exemplary plant **700**, it is assumed that the combined power capacity of the microsources **755** and **765** is not adequate to supply the total load from loads M**5**, M**8**, M**7**, and M**9**. However, the combined power capacity of the microsources **755** and **765** is adequate to supply the combined load from loads M**5**, M**8**, and M**9**, which are assumed to be critical loads. For this reason, when the exemplary plant **700** transfers to island mode by opening switch **725**, the second switch **732** can also be opened to disconnect feeder **745** and its associated load M**7** from the main distribution bus **730**.

FIGS. **10**(*a*), **10**(*b*), and **10**(*c*) are graphs of predicted regulated voltages on bus **738**, bus **739**, and the external side **747** of the switch **725** at the 13.8 kV feeder, respectively, during a transfer to island mode by opening both switch **725** and switch **732** in response to a loss of power from the 13.8 kV feeder.

At t=10 seconds, the system moves from grid-connected to island operation by opening switch **725** to disconnect the plant **700** from the feeder **710** in response to the loss of power from the 13.8 kV feeder (where graph **1020** flattens). At the same time, the non-critical feeder **745** and its associated load M**7** is disconnected from the remainder of the plant **700** by opening switch **732**. Waveforms for bus **738** and **739** voltages during the switch to island mode are shown in graphs **1000** and **1010** in FIGS. **10**(*a*) and **10**(*b*), respectively. As shown in the graph, there is only a slight change from the sinusoidal steady state after t=10 seconds and the change lasts less than a cycle.

FIGS. **11**(*a*) and **11**(*b*) are graphs of predicted real power and reactive power, respectively, of the microsources **755** (P**8**) and **765** (P**9**) in the exemplary industrial plant of FIG. **7** during a transfer to island mode by opening both switch **725** and switch **732**. Real power has to take up the critical load in the absence of grid power. Upon islanding, both microsources **755** and **765** increase their power injection as expected from the design of the droop characteristics. Microsource **765** is assumed to serve a lighter load M**9** on bus **739**.

As seen in the graph **1110**, the power output of microsource **765** increases more than the power output of microsource **755** in response to the islanding, so microsource **765** is picking up the largest part of the new load demands. Reactive power injection reduces but holds the voltages at 1 pu. Power regulation takes place very rapidly, and steady-state power is restored in less than one second. In this case, system frequency droops a little more than 0.5 Hz.

As described with reference to FIGS. **1-11**, a local controller at each microsource can insure stable operation in an electrical distribution system. This controller can respond in milliseconds and use local information to control the microsource during all system or grid events. Advantageously, communication among microsources is not necessary for basic system operation; each inverter is able to respond to load changes in a predetermined manner without data from other sources or locations. This arrangement enables microsources to "plug and play." That is, microsources can be added without changes to the control and protection of units that are already part of the system.

Control schemes for a power controller in a system of distributed energy resources (DER), such as the power controller **340** in FIG. **3**, can be classified into one of three broad classes: unit power control, zone power control, and a mixed system using both unit power control and zone power control. FIGS. **12-18** depict aspects of unit power control, and FIGS. **19-23** depict aspects of zone power control. FIGS. **24-29** depict simulations of unit power control, FIGS. **30-33** depict simulations of zone power control, and FIGS. **34-36** depict simulations of mixed unit and zone power control.

FIG. **12** shows a basic unit power controller in accordance with an exemplary embodiment of the invention, based on [Eq. 8] below:

$$\omega_i=\omega_0-m(P_0-P_{meas}) \qquad \text{[Eq. 8]}$$

Note that the input δ_E in FIG. **3**, is not needed in the basic unit power controller according to the exemplary embodiment. This basic unit power controller uses a set point unit power flow P_0 and the measured power P_{meas} to control the instantaneous operating frequency ω_i of the inverter by changing the operating phase angle of the inverter $\delta_v(t)$.

FIG. **13** is a diagram of an exemplary microgrid that includes a microsource with unit power control in accordance with an exemplary embodiment of the invention. The exemplary microgrid **1300** includes a local power bus **1310**, at least one microsource **1320** connected to the power bus **1310** by an inductor **1315**, and at least one load **1330**. A switch **1340** may be provided, for example in the local power bus **1310**. The switch **1340** can be opened to isolate the microgrid **1300** from the rest of the system **1345**, which may include a utility grid **1350**, and the switch **1340** can be closed to connect the microgrid **1300** to the rest of the system **1345**. The microsource **1320** may include a controller able to measure a current through the inductor $\bar{I}$ and a system voltage $\bar{E}$ measured at the point **1325** where the inductor **1315** joins the power bus **1310**.

When the microgrid of FIG. **13** is connected to the grid, load changes are matched by a corresponding power injection from the utility. This is because the unit holds its injection to a set point P_0. During island mode all the units participate in matching the power demand as loads change. Either a variable slope method or a fixed slope method can be used in a preferred embodiment of a unit power controller according to the invention. In either case the characteristics are described by [Eq. 8].

FIG. **14** is a graph depicting the relationship between steady state unit power vs. frequency (P-ω) in a variable slope method for use in unit power control, for two exemplary microsources having different power set points. This is called a variable slope method because different microsources in the system can have different operating characteristics, each with its own slope that depends on the magnitude of its power set point.

In this example, the two microsources have different power set points, P_{o1} and P_{o2}. When the microsources are connected to the grid, they produce power according to these respective power set points, P_{o1} and P_{o2}, and they both operate at the same nominal frequency ω_o. If the microsources were importing power from the grid before islanding, the two microsources both increase their power outputs when the system islands, by reducing their operating frequency. For the case where the microgrid was exporting power to the grid the power needs to be reduced when the system islands, resulting in a frequency increase.

The slope 'm' is variable, and for each microsource is a function of the power set point, P_o and the maximum power output, P_{max}, of that microsource according to [Eq. 9]:

$$m=\frac{2\pi\Delta f}{(P_o-P_{max})} \qquad \text{[Eq. 9]}$$

The higher the power set point, the steeper is the slope. By construction, maximum power is reached at minimum frequency in all units. During grid mode the system operates at system frequency, ω_o, and the output power of each microsource unit matches its corresponding power setpoint, P_{o1} and P_{o2}. During island mode the units must provide all the power for the loads.

If the units were importing from grid prior to transfer to island, then the units will ramp up their output to match the load's demand, by decreasing their instantaneous frequency until they reach steady state operating points, shown in FIG. **14** with circles at the resulting lower steady state frequency, ω_{imp}.

Similarly, If the units were exporting from grid prior to transfer to island, then the units will decrease their output to match the load's demand, by increasing their instantaneous frequency until they reach steady state operating points, shown in FIG. **14** with circles at the resulting higher steady state frequency, ω_{exp}.

If the units were exporting even more power, the theoretical steady state operating frequency could be an even higher frequency, ω_{over}. At this higher frequency, ω_{over}, the output power and operating frequency of the microsources could be outside their range of normal operation. For example, at an operating frequency ω_{over}, unit **1** could be below its minimum power range and above its maximum frequency range. Similarly, at an operating frequency ω_{over}, unit **2** could be above its maximum frequency range, although within its power range.

One characteristic of the variable slope method is that all units reach their maximum power output and their minimum frequency limit simultaneously. This is because the operating characteristics for all the units converge at the point of maximum power and minimum frequency. Although the units may reach steady state operating points having different output power levels, they will in general reach the same steady state operating frequency at any given time.

One of the advantages of the variable slope method is that all sources reach their maximum output together and there are no problems with limits on minimum frequency or maximum power. The use of variable slopes allows the power to increase more in the units that are less loaded (unit **1**) and increase less in the units that are more loaded (unit **2**).

If the system is engineered such that the combined power capacity of all the microsources in the system exceeds the maximum combined load in the system, then that total load can be matched with all the units injecting less than maximum power. In such a case, there is no need to enforce any limit on maximum power unless the load exceeds the aggregate power capacity of the units. All the units would reach maximum power at the same frequency, at about the same time.

The frequency corresponding to maximum power for all the units is the lower limit for the frequency range, $\omega_o-\Delta\omega$. Since all units cannot exceed maximum power, as seen before, then it follows that the units will not go beyond the lower limit for the frequency range.

One potential problem with this variable slope approach is that the minimum power limit, P_{min}, could be exceeded (see squares at frequency ω_{over} in FIG. **14**) and a limit controller is needed to avoid it. Overfrequency is another potential problem with this variable slope approach. As shown in FIG. **14**, it is possible to reach a steady state at a frequency ω_{over} that is larger than the maximum limit for the frequency, $\omega_o+\Delta\omega$ and there is no mechanism to prevent that.

FIG. **15** is a graph depicting the relationship between steady state unit power vs. frequency (P-ω) in a variable slope method with power and frequency limits for use in unit power control, for two exemplary microsources having different power set points. During operation below the maximum frequency and above the minimum power limit of each microsource, the slope is variable and depends on the power set point, P_o and the maximum power output, P_{max}, of that microsource according to [Eq. 8], as in the scheme of FIG. **14**.

In this approach, the steeper slopes are switched to a flatter characteristic. The change of slope could occur at any frequency between ω_o and $\omega_o+\Delta\omega$. The flatter characteristics will all have P=0 at maximum frequency. The change of slope is performed for all the power set points P_{oi} larger than half of maximum power P_{max}. This setpoint ($P_{oi}=P_{max}/2$) is shown with a dashed thick line on FIG. **15**.

Like in the preceding case, power imported from the grid implies a lowering of the frequency in island, to a value like ω_{imp}. If power was exported while connected to grid, then in island the frequency would increase to ω_{exp}. The value of this new frequency depends on how the characteristic is switched from steep to flatter.

If the slope is switched at any intermediate frequency between nominal and maximum limit, then the operating point would be at a frequency like ω_{exp} in FIG. **15**, with the operating points shown as circles. In this case the flatter part of the slope has a non zero rate of change.

If the slope is switched at the maximum frequency, then the flatter part of the slope has zero rate of change: it is horizontal. In this condition the operating points will result to be at this frequency (the maximum frequency that is held) and are shown with squares on FIG. **15**. Notice that this power dispatch equals exactly the power dispatch that was previously obtained at the frequency ω_{exp}.

The maximum power limit is automatically enforced for the same reasons already seen when analyzing the characteristics in FIG. **14**. The minimum power limit is enforced differently depending on whether the power set point P_{oi} is above or below half the maximum power capacity P_{max} of the microsource.

If $P_{oi}<P_{max}/2$, then there is no switch to a flatter slope (like for unit **1**). In this case the steady state characteristic is switched to vertical slope as soon as P=0. The steady state operation is constrained to belong to this vertical part of the characteristic: as the load decreases, frequency increases at a constant power, P=0, as shown by the arrow in FIG. **15**.

If $P_{oi}>P_{max}/2$, then the slope is switched to a flatter slope (potentially horizontal). No matter what is the slope of the flatter part, all characteristics will reach the operating point at P=0 and maximum frequency, moving in the direction of the arrows (FIG. **15**) as load decreases.

Minimum frequency limit cannot be exceed as a consequence of the fact that maximum power cannot be exceeded. Indeed, the only way that the minimum limit on frequency can be exceeded is if the limit on maximum power is also exceeded, i.e. there are more loads than generation in the microgrid.

Maximum frequency limit cannot be exceeded because of the same reasons the minimum cannot be exceeded. Any higher frequency that this limit would imply that the loads are actually injecting power into the system.

This approach correctly enforces the limits on the frequency and the power. At higher setpoints, the slope could became very steep at the point of compromising stability The problem of stability could be solved by assigning a maximum slope that the characteristic is allowed to have Since the slope is a function of the power setpoint, then this would effectively translate into a limit on the maximum power setpoint. Microsources are expected to operate most of their time with power outputs near maximum because of the better efficiencies enjoyed at higher operating points. Limiting the maximum power that can be injected during grid connection still implies that during island the unit may end up operating at full maximum power. (i.e. suppose that P_{o2}, its max power setpoint, then in island at frequency ω_{imp} power output would be larger than P_{o2} and it could go up to P_{max}, if loads increase, without problems).

FIG. **16** is graph depicting the relationship between steady stat unit power vs. frequency (P–ω) in a fixed slope method for use in unit power control, for two exemplary microsources having different power set points. In the approach of FIG. **16**, the slope of the steady state characteristic is held constant so this control characteristic is called "fixed slope."This fixed slope can be steeper than the minimum slope (see [Eq. 10]). This minimum value is defined by the fact that frequency will change by Δω as power changes by ΔP (the approach using the minimum slope is dealt in FIG. **17**).

Power set points are tracked in grid mode, and upon islanding the frequency readjusts up or down as already seen. For instance, if power was being imported from the grid in grid mode, after islanding the frequency of each microsource will drop below ω_o to ω_{imp} as the units supply the power that was injected by the grid before islanding. Unlike the approach with the variable slope, each unit increases output power to meet the power demand the same amount, regardless of their respective power set points before islanding.

A steady state horizontal characteristic is enforced at maximum and minimum frequencies allowing power to change at those frequencies. The slanted characteristics are only valid within limits of power and frequency, the part outside of the limits (dashed lines) are replaced with the horizontal steady state characteristics to enforce frequency limits. For instance if the system in island is operating at frequency ω_{imp} and the load suddenly increases, then the operating point may end up at the minimum frequency, represented by the squares. The steady state operating points would move on the characteristic, following the arrows (FIG. **16**) as load increases.

The case where the system was exporting to grid would lead to frequency ω_{exp} in island, and a lower load may bring operation to the maximum frequency, shown with squares.

Maximum and minimum frequencies can be reached, but the fact that the characteristic with constant slope is switched to horizontal at those frequencies prevents any operation point from ever exceeding the limits. Maximum and minimum output power is enforced by ensuring that the steady state characteristics do not extend over these limits: for instance, the operating point at maximum frequency for unit **1** is P=0 is held fixed unless the load increases.

This steady state characteristic configuration has the advantage of being stable across its range (as long as the slope is not chosen too large) and of enforcing both limits on power and frequency. The only disadvantage is that both limits in frequency and power need to be actively enforced. In contrast, in the method of FIG. **15** the limit P_{max} was automatically enforced by assuming enough generation and the limit on the minimum frequency also was inherently enforced because of the fact that power could not exceed maximum.

FIG. **17** is a graph depicting the relationship between steady state unit power vs. frequency (P-ω) in a fixed minimum slope method for use in unit power control, for two exemplary microsources having different power set points;

$$m = -\frac{\Delta\omega}{P_{max}} \quad \text{[Eq. 10]}$$

This slope allows power to change between P=0 and $P=P_{max}$ as frequency changes by Δω, shown in FIG. **17** with the thick dashed line. All the other characteristics are simply parallel to this one. If the system was importing from the grid before islanding, then the resulting frequency, ω_{imp} will be smaller than the system frequency ω_o, as already seen. It is possible that one of the units reaches maximum power in island mode, as shown by unit **2** at frequency ω_{imp}.

The steady state characteristic slope switches to vertical as soon as the maximum power limit has been reached and the operating point moves downward vertically as shown by the arrows in FIG. **17** as load increases. Opposite considerations take place when unit is exporting and new frequency ω_{exp} is larger than nominal. It is possible that if the load is very small that one of the units has reached the limit P=0. At that point, the slope of the characteristic is switched to vertical and as load decreases, the operating point moves upwards, as shown by the arrows in FIG. **17**.

The minimum and maximum power limits are enforced by the fact that the characteristics with const slope are switched to vertical steady state characteristics. The minimum and maximum frequency limits cannot be overshot because it would imply, respectively, that the load has exceeded the overall generation capability or that the load is actually injecting power into the system. These last two limits do not need to be explicitly enforced since the assumption on the load (smaller than sum of all generation, but never smaller than zero) automatically implies behavior within limits.

FIG. **18** is a diagram of a unit power controller with upper and lower power limits in accordance with an exemplary embodiment of the invention. This approach has the advantage of being able to enforce both limits in power and frequency. For the fixed minimum slope only power limits need to be enforced, frequency limits come as a consequence.

FIG. **19** is a diagram of a microgrid containing an exemplary microsource with zone power control in accordance with an exemplary embodiment of the invention. The exemplary microgrid **1900** includes a local power bus **1910**, at least one microsource **1920** connected to the power bus **1910** by an inductor **1915**, and at least one load **1930**. A switch **1940** may be provided, for example in the local power bus **1910**. The switch **1940** can be opened to isolate the microgrid **1900** from the rest of the system, which may include a utility grid **1950**, and the switch **1940** can be closed to connect the microgrid **1900** to the rest of the system. The microsource **1920** may include a controller able to measure a system voltage $\overline{E}$ where the microsource **1920** is connected to the local power bus **1910**, and a current $\overline{I}_{feeder}$ between the local power bus **1910** and the rest of the system **1945**, measured at the point **1925**.

Zone power control is another way to control the power in a system of DERs, by controlling power flow in zones instead of by controlling the power flow from each microsource. To reduce confusion we use the symbol, F, for power flow in a zone and P for the output of a source. FIG. **19** shows the setup: when connected to the grid, every load change is matched by a different power injection from the unit since the control holds the flow of power coming from the grid, F_{line}, to a constant value. During island mode all the units participate in matching the power demand as loads change.

FIG. **20** is a graph depicting the relationship between steady state zone power vs. frequency (P-ω) in a method for use in zone power control, for two exemplary microsources having different power set points. The characteristics enforce the following relation:

$$\omega_i=\omega_o-m_F(F_{o,i}-F_i) \quad \text{[Eq. 11]}$$

This expression is very similar to [Eq. 8] used for unit output power control. The slope is fixed at the minimum slope, [Eq. 10], but has a reversed sign (m_F=−m, the characteristics are slanted the opposite way). The sign needs to be reversed because of the relation between the output power, P and the zone flow F. This relation can be derived by inspection of FIG. **17**:

$$F_{line}+P_{source}=\text{Load} \quad \text{[Eq. 12]}$$

In [Eq. 12], F_{line} is the power (imported means positive) from the rest of the system, and P_{source} is the power injected or absorbed by the unit. The power injected or absorbed by the unit is assumed to be greater than the minimum power output of the unit, P_{min}, and less than the maximum power output of the unit, P_{max}. For a microsource capable of power injection only P_{min} will be positive or zero, while a bidirectional device capable of both power injection or power storage may have $P_{min}<0$. Load is the overall loading level seen by the unit. The relationship of [Eq. 12] implies that to increase F one needs to decrease P and vice versa, hence the reverse sign in the slope when moving from the P−ω plane to the F−ω plane.

During connection with the grid the flows in the zones track the requested values, F_{oi}, at the system frequency, ω_o. When the microgrid transfers to island, the two units readjust the flow dispatch depending on the geometrical configuration of the units in the field.

FIGS. **21** and **22** are diagrams of two microsources installed in a single zone and in two zones, respectively. The use of two microsources in a single zone in FIG. **21** is for illustrative purposes only, and there can be a greater or lesser number of microsources in a single zone. Similarly, the use of two zones each with a single microsource in FIG. **22** is also for illustrative purposes only, and there can be a greater or lesser number of zones, and the number of microsources in each zone may be different.

FIG. **21** shows a single-zone microgrid **2100** having two microsources **2102** and **2105**, and two loads **2104** and **2106** on a local power bus **2103**, and connected by an interface switch **2101** to a utility system **2107**. FIG. **22** shows a two-zone microgrid **2200** having a first zone with a microsource **2202** and a load **2204** on a first local power bus **2203** and a second zone with a microsource **2205** and a load **2206** on a second local power bus **2207**, with the microgrid **2200** connected by an interface switch **2201** to a utility system **2208**.

In a zone control method for the circuit of FIG. **21**, during island the switch **2101** will open, so the flow nearest to utility must be zero. FIG. **20** shows that flow of unit **1** is the one nearest to the utility, so in island the system will operate at the frequency ω_1, where flow of unit one is zero. The operating points are shown with squares at that frequency. Frequency ω_1 is larger than the nominal system frequency because the system was exporting to the grid (F_{o1} is negative) prior to disconnection, which is the same behavior seen with unit output power control. If, for instance, the two characteristics of FIG. **21** are swapped (i.e. replace $F_{o1(new)}=F_{o2(old)}$ and $F_{o2(new)}=F_{o1(old)}$), then the frequency in island would be ω_2. This time the frequency is lower than nominal, and that is because the microgrid was importing from the grid prior disconnection.

In a zone control method for the circuit of FIG. **22**, during island the frequency takes the value where the sum of the flows is zero. On FIG. **20**, the frequency in island is ω_3, exactly where F**1**=–F**2**. The operating points are shown with triangles at that frequency.

So far it was assumed that all the units operate within their limits of power and frequency. As seen in FIG. **17**, the choice of the minimum slope value guarantees operation within frequency limits across the whole operating range of output power but it requires the unit output power limits to be actively enforced. The limits on output power variable, P, are projected on the zone flow variable, F, as shown in FIG. **23**. These regions slide as the loads change their operating points. But in all cases a unit must operate between its maximum and its minimum power points.

FIG. **23** is a graph depicting the relationship between steady state zone power vs. frequency (P-ω) in a method with unit power limits for use in zone power control, for two exemplary microsources having different power set points. FIG. **23** shows unit **1** during island operation will operate at frequency ω_1, where flow F_1 is zero. And the output of unit **2** has reached its zero limit. Note solid squares on the ω_1 line. Of course this implies that unit one is providing all needed power. The islanding events at ω_2 & ω_3 show the enforcement of maximum power limits.

FIG. **24** is a diagram of a zone power controller with upper and lower unit power limits in accordance with an exemplary embodiment of the invention. The controller for zone power flow of FIG. **24** is almost identical to the unit power controller of FIG. **18**. The differences are in gain and inputs. First, the slope, m, in the zone power controller of FIG. **24** is negative relative to the slope, m, in the unit power controller FIG. **18**. Second, the zone power controller of FIG. **24** takes as inputs the zone power flow set point, F_o, and measure zone power flow, F_{meas}.

The upper and lower unit power limits P_{min} and P_{max} are still required in a zone power controller, since the unit power limits must be enforced. The limits are enforced by injecting a Δω offset when a limit is reached, for the maximum power limit $\Delta\omega \leqq 0$, while for the minimum power limit, $\Delta\omega \geqq 0$. When the system is not at a limit $\Delta\omega=0$. Note that the limiters assume that the power measurement can become negative. The control scheme of FIG. **24** will allow both methods of operation provided the external inputs are available.

From an installation perspective several items may need to be set externally; value of m including its sign, maximum and minimum power values of the unit, gains in limiters, and the value of ω_o. The power flow set point needs to be part of the energy management system (EMS).

FIGS. **25-29** depict computer and hardware simulations of unit power control of the exemplary system of FIG. **21** which includes two microsources arranged in a single zone. These simulations show the behavior of the system of FIG. **21** when operated using the fixed value, minimum slope approach shown in FIG. **17** and subjected to load changes that cause the microsources to reach their limits.

When all the units control output power, then the quantities P**1** and P**2** are controlled. When all the units control zone flow, then the quantities F**1** and F**2** are controlled. In a mixed system that includes both unit power control and zone power control, it is necessary to specify which unit controls P and which controls F.

FIGS. **25**(*a*) and **25**(*b*) are graphs of predicted output power and instantaneous frequency, respectively, from the microsources in the exemplary system of FIG. **21**, from a computer simulation of unit power control of the system of FIG. **21** during the following sequence of events:

t = 0 sec	steady state, grid connected	operating at steady state A
t = 1 sec	transfer to island	transition to steady state B
t = 3 sec	first load inserted	transition to steady state C
t = 5 sec	second load inserted	transition to steady state D
t = 7 sec	third load inserted	transition to steady state E
t = 10 sec	third load removed	transition to steady state D
t = 12 sec	second load removed	transition to steady state C

FIG. **25**(*a*) shows the output power from both units. In FIG. **25**(*a*), in this case power is normalized and displayed "per unit" or "pu", mapping the operating range [0, P_{max}] to the interval of [0, 1.0]. Power never exceeds the maximum value of 1.0 per unit in steady state. All the steady states have been labeled with capital letters corresponding to the steady states listed above.

FIG. **25**(*b*) shows the instantaneous frequency at both units as the system is subject to the same events. The value of Δω, needed to calculate the value of the slope, has been chosen to correspond to a maximum frequency deviation of 0.5 Hz, but this particular value is chosen for illustration and not as a limitation. Other maximum frequency deviations greater than or less than 0.5 Hz could be used.

The simulation of FIGS. **25**(*a*)-(*b*) shows a unit reaching maximum output as a consequence of load increasing. If the load was actually decreased, then it follows that one of the two units will reach zero power output limit.

FIGS. **26**(*a*) and **26**(*b*) are graphs of predicted output power and instantaneous frequency, respectively, from the microsources in the exemplary system of FIG. **21**, from a computer simulation of unit power control of the system of FIG. **21** during a different sequence of events:

t = 0 sec	steady state, grid connected	operating at steady state A
t = 1 sec	transfer to island	transition to steady state B
t = 3 sec	first load removed	transition to steady state F
t = 5 sec	second load removed	transition to steady state G
t = 8 sec	second load inserted	transition to steady state F
t = 10 sec	first load inserted	transition to steady state B

FIG. **26**(*a*) shows the output power from both units during the sequence of events above. All the steady states have been labeled with capital letters corresponding to the steady states listed above. FIG. **26**(*b*) shows the instantaneous frequency at both units as the system is subject to the same events. Active power injection never falls below the value of P_{min}=0 pu in steady state. On FIGS. **26**(*a*)-(*b*), steady states A and B are the same as in FIGS. **25**(*a*)-(*b*).

FIG. **27** is a graph depicting the relationship between steady state unit power vs. frequency (P-ω) in a method of unit power control of the system of FIG. **21**, showing the steady state operation points (A)-(G) of FIGS. **25**-**26** for both units. FIG. **27** shows that the operating points (A)-(G) fall on the steady state characteristics of a unit control scheme such as that of FIG. **17**.

FIGS. **28**(*a*) and **28**(*b*) are graphs of predicted real power (P) and reactive power (Q) from the microsources of unit **1** and unit **2**, respectively, in the exemplary system of FIG. **21**, from a hardware simulation of unit power control of the system of FIG. **21** when a new load is inserted during the following sequence of events:

t = 0 sec	steady state, island mode	operating at steady state A
t = t_1 sec	load is inserted	transition to steady state B

The results of the hardware simulation of the system of FIG. **21** are very similar to the results of the computer simulation of that system. The loading event at t=t_1 sec is designed so that the load insertion leads unit **1** to reach its maximum power output.

Notice that the power scaling is such that the interval is projected on a corresponding interval of [**0**, **0.8**]. The value 0.8 pu represents maximum power. This is because of the issues of representing quantities in hardware. Namely, the Digital Signal Processor used was only able to represent numbers between −1 and +1. If 1.0 was used to represent maximum power, it would not be possible to represent any overshot (i.e., any power in excess of the maximum power). With P_{max} being 0.8, then small overshoots larger than P_{max} can be internally represented.

FIGS. **29**(*a*) and **29**(*b*) are graphs of predicted real power (P) and reactive power (Q) from the microsources of unit **1** and unit **2**, respectively, in the exemplary system of FIG. **21**, from a hardware simulation of unit power control of the system of FIG. **21** when a load is removed during the following sequence of events:

t = 0 sec	steady state, island mode	operating at steady state C
t = t_2	load is removed	transition to steady state D

The load removal event at t=t_2 sec is designed so that the load insertion leads unit **2** to reach its minimum power output, P=0. Notice that the initial steady state points A and C are not identical. The power setpoints are the same, but the loading level is different: higher in A (so that a load insertion allows to reach Pmax), lower in C (so that a load removal allows to reach P=0). Although there is no available frequency waveform, these hardware results show that the power in steady state is constrained to the interval [0, P_{max}] (i.e. [0, 0.8]) exactly as shown in FIG. **17**.

FIGS. **31**-**33** depict computer simulations of zone power control of the exemplary system of FIG. **30** having two zones, an upper zone with two microsource units, and a lower zone with one microsource unit.. The two-zone microgrid **3000** of FIG. **30** has a first zone with a microsource **3002** and a load **3004** on a first local power bus **3003** and a second zone with microsources **3005** and **3008** and loads **3006** and **3009** on a second local power bus **3007**, with the microgrid **3000** connected by an interface switch **3001** to a utility system **3010**.

These simulations show the behavior of the system of FIG. **30** when operated using the zone control approach shown in FIG. **20** and subjected to load changes that cause the microsources to reach their limits when all the units are controlling the zone power flow. No hardware results are shown for this control configuration.

The earlier description in (0132 -0156) showed that there are several events that could lead to units reaching their limits. On the F−ω plane the limits were shown as a sliding window. The window slides as loads change: in this simulation no load will be changed to ensure that the window will stay motionless. This is to ease the inspection of the plots, but does not limit the scope of the results.

FIGS. **31**(*a*) and **31**(*b*) are graphs of predicted zone power flow and instantaneous frequency, respectively, from the microsources in the exemplary system of FIG. **30**, obtained using a computer simulation of zone power control during a sudden transfer to island mode from a steady state connected to the grid. This transfer to island triggers one of the units to reach one of its limits.

t = 0 sec	steady state, grid connected	operating at steady state A
t = 1	transfer to island	transition to steady state B

FIG. **31**(*a*) shows the flow in each of the controlled zones following the islanding. During grid connection the setpoints F_{o1} through F_{o3} are tracked. When grid disconnects, the sum of the flows that converge to the grid must be zero. From FIG. **24**, this implies F**1**=−F**3**, which is the condition established during island mode. FIG. **31**(*b*) shows that the frequency is increased from the nominal system value to a higher value when the system islands.

FIG. **32**(*a*) is a graph depicting the relationship between steady state frequency vs. zone power flow in a method of zone power control of the system of FIG. **30**, showing the steady state operation points (A)-(B) of FIGS. **31**(*a*)-**31**(*b*). FIG. **32**(*b*) is a magnification of FIG. **32**(*a*) from operating point (A) to operating point (B) for unit **2**.

Unit **2** reaches minimum power and is constrained on the vertical portion of the steady state characteristic, as shown magnified in FIG. **32**(*b*). Notice that since units **1** and **3** are operating within their limits, then their steady state points will belong to the slanted part of the steady state characteristic, as expected. To avoid confusion, only the operating window of unit **2** is shown. Since the steady state point B lays on the vertical band delimiting the right side of the window, then it must be that a minimum power limit is reached.

FIG. **33** is a graph of the predicted unit real power flow from the microsources in the exemplary system of FIG. **30**, obtained using a computer simulation of zone power control during a transfer to island mode. FIG. **33** shows that unit **2** reaches a P=0 limit, as expected.

FIGS. **34**-**36** depict computer simulations of a mix of unit and zone power control of the exemplary system of FIG. **30** having two zones, an upper zone with two microsource units, and a lower zone with one microsource unit. In a mix of zone and unit power control, in which some of the units control unit output power while others control zone power flow:

Unit 1	Zone Flow Control	zone flow setpoint F_{o1}
Unit 2	Unit Output Control	unit power setpoint P_{o2}
Unit 3	Zone Flow Control	zone flow setpoint F_{o3}

For the units controlling zone power flow, the limits are shown on the F-ω plane as a sliding window. The window slides when loads change: no load will be changed to ensure that for this experiment the window will stay motionless. This is to ease the inspection of the plots, but does not limit the scope of the results.

These computer simulations show the behavior of the system of FIG. **30** when operated using the above-described mix of zone and unit power control, when the system is subjected to the following events:

t = 0 sec	steady state, grid connected	operating at steady state A
t = 1	Transfer to island	transition to steady state B

FIGS. **34**(*a*) and **34**(*b*) are graphs of predicted zone power flow and instantaneous frequency, respectively. FIG. **34**(*a*) shows the zone flows as the system transfers to island. The setpoints for units **1** and **3** are tracked during grid connection. The flows F**1** and F**3** are constrained by the steady state characteristic, while the flow F**2** is just a measure and is not subject to any constraint. Because the sum of the flows to the grid must equal zero in island, then from FIG. **24**, it follows that F**1**=−F**3**, which can be visually verified in FIG. **34**(*a*). FIG. **34**(*b*) shows the frequency during the same event: it has decreased from the nominal value.

FIG. **35** is a graph of the predicted unit real power flow from the microsources in the exemplary system of FIG. **30**, obtained using a computer simulation of a mix of zone and unit power control during a transfer to island mode. Note that the setpoint output power for unit **2** is tracked during grid connection. During islanding the value of P**2** is constrained by the steady state characteristic (FIG. **17**), while P**1** and P**3** are just measures of the injections and are not constrained to a characteristic. FIG. **35** shows that the transfer to island causes unit **3** to reach maximum output power, while units **1** and **2** are within limits.

FIG. **36** is a graph depicting the relationship between steady state frequency vs. zone and unit power flow in a method of mixed zone and unit power control of the system of FIG. **30**, showing the steady state operation points (A)-(B) of FIGS. **34**(*a*)-**34**(*b*), and FIG. **35**. Notice that this is a mixed (P-ω and F-ω) plane. Unit **3** reaches maximum and is constrained on the vertical portion of the steady state characteristic. Notice that since unit **1** is operating within its limits, then its steady state will belong to the slanted part of the steady state characteristic, as expected. Unit **2** (that regulates P) is also within limits and its steady state points lay inside its own operating window.

The fact that unit **3** reaches a maximum power limit explains why the steady state lays on the left side vertical portion of the characteristic. FIG. **36** shows only the limits relevant to unit **3** to avoid confusion when overlapping the limits of all three units.

It is important to note that the construction and arrangement of the steps in the methods, and the elements of the structures, shown in the exemplary embodiments discussed herein are illustrative only. Those skilled in the art who review this disclosure will readily appreciate that many modifications are possible (e.g., variations in sizes, dimensions, structures, shapes and proportions of the various elements, values of parameters, mounting arrangements, materials, transparency, color, orientation, etc.) without materially departing from the novel teachings and advantages of the invention.

The order or sequence of any process or method steps may be varied or re-sequenced according to alternative embodiments. Other substitutions, modifications, changes and/or omissions may be made in the design, operating conditions and arrangement of the preferred and other exemplary embodiments without departing from the spirit of the present invention as expressed in the appended claims.

The components of the invention may be mounted to each other in a variety of ways as known to those skilled in the art. As used in this disclosure and in the claims, the terms mount and attach include embed, glue, join, unite, connect, associate, hang, hold, affix, fasten, bind, paste, secure, bolt, screw, rivet, solder, weld, and other like terms. The term cover includes envelop, overlay, and other like terms.

While the exemplary embodiments illustrated in the figures and described above are presently preferred, it should be understood that these embodiments are offered by way of example only. Other embodiments may include, for example, different techniques for power calculation, voltage control, power control, or droop control. The invention is not limited to a particular embodiment, but extends to various modifications, combinations, and permutations that nevertheless fall within the scope and spirit of the appended claims.

It is understood that the invention is not confined to the embodiments set forth herein as illustrative, but embraces all such forms thereof that come within the scope of the following claims.

What is claimed is:

1. A method of controlling distributed energy resources, the method comprising:

providing a microsource, wherein the microsource is located in a microgrid, and further wherein the micro source is configured to deliver a power P**1** at a frequency ω1;

operating the microsource in a grid mode in which the microsource is connected to a utility grid, wherein during operation in the grid mode the frequency ω1 is approximately equal to a frequency ω_o and the power P**1** is equal to a power $P1_o$, wherein the frequency ω_o is an operating frequency of the utility grid; and

transferring the microsource from the grid mode to an island mode such that the microsource is disconnected from the utility grid, wherein ω1 is equal to ω_{island} and P1 is equal to $P1_{island}$ during the island mode;

wherein $\omega_{island} > \omega_0$, and $P1_{island} < P1_0$ if the microgrid was exporting power prior to the transfer from the grid mode to the island mode;

wherein $\omega_{island} < \omega_0$, and $P1_{island} > P1_0$ if the microgrid was importing power prior to the transfer from the grid mode to the island mode; and

wherein the microsource delivers a maximum power output level $P1_{max}$ at a frequency ω_{min}, wherein the microsource has a slope switch frequency ω_{switch}, and

$$\omega_{island} \approx \omega_0\left(\frac{\omega_0 - \omega_{min}}{P1_0 - P1_{max}}\right)(P1_0 - P1_{island}).$$

$$\text{if } \left[\omega_0 - \left(\frac{\omega_0 - \omega_{min}}{P1_0 - P1_{max}}\right)(P1_0 - P1_{island})\right] < \omega_{max}.$$

2. The method of claim **1**, wherein the microsource delivers a maximum power output level $P\mathbf{1}_{max}$ at a frequency ω_{min}, and wherein

$$\omega_{island} \approx \omega_0\left(\frac{\omega_0 - \omega_{min}}{P2_0 - P2_{max}}\right)(P2_0 - P2_{island}).$$

3. The method of claim **1**,

$$\text{wherein } \omega_{island} \approx \omega_0 - \left(\frac{\omega_0 - \omega_{min}}{P1_0 - P1_{max}}\right)(P1_0 - P1_{island})$$

$$\text{if } \left[\omega_0 - \left(\frac{\omega_0 - \omega_{min}}{P1_0 - P1_{max}}\right)(P1_0 - P1_{island})\right] \geq \omega_{switch}.$$

4. The method of claim **1**, wherein the microsource delivers a maximum output level $P\mathbf{1}_{max}$ at a frequency ω_{min} wherein the microsource has a maximum operating frequency ω_{max},

$$\text{wherein } \omega_{island} \approx \omega_0 - \left(\frac{\omega_0 - \omega_{\min}}{P1_0 - P1_{\max}}\right)(P1_0 - P1_{island})$$

$$\text{if } \left[\omega_0 - \left(\frac{\omega_0 - \omega_{min}}{P1_0 - P1_{max}}\right)(P1_0 - P1_{island})\right] < \omega_{max}; \text{ and}$$

wherein

$$\omega_{island} \approx \omega_{max} \text{ if } \left[\omega_0 - \left(\frac{\omega_0 - \omega_{min}}{P1_0 - P1_{max}}\right)(P1_0 - P1_{island})\right] \geq \omega_{max}.$$

5. The method of claim **1**, wherein the microsource delivers a maximum power output level $P\mathbf{1}_{max}$ at a frequency ω_{min}, wherein the microsource has a slope switch frequency ω_{switch}, wherein the microsource has a maximum operating frequency ω_{max},

$$\text{wherein } \omega_{island} \approx \omega_0 - \left(\frac{\omega_0 - \omega_{min}}{P1_0 - P1_{max}}\right)(P1_0 - P1_{island})$$

$$\text{if } \left[\omega_0 - \left(\frac{\omega_0 - \omega_{min}}{P1_0 - P1_{max}}\right)(P1_0 - P1_{island})\right] < \omega_{switch};$$

$$\text{wherein } \omega_{island} < \omega_0 - \left(\frac{\omega_0 - \omega_{min}}{P1_0 - P1_{max}}\right)(P1_0 - P1_{island})$$

$$\text{if } \omega_{switch} \leq \left[\omega_0 - \left(\frac{\omega_0 - \omega_{min}}{P1_0 - P1_{max}}\right)(P1_0 - P1_{island})\right] < \omega_{max}; \text{ and}$$

wherein

$$\omega_{island} \approx \omega_{max} \text{ if } \left[\omega_0 - \left(\frac{\omega_0 - \omega_{min}}{P1_0 - P1_{max}}\right)(P1_0 - P1_{island})\right] \geq \omega_{max}.$$

6. The method of claim **1**, wherein the microsource delivers a maximum power output level $P\mathbf{1}_{max}$ at a frequency ω_{min}, wherein the microsource has a minimum power output level $P\mathbf{1}_{min}$,

wherein

$$P1_{island} \approx P1_0 - \left(\frac{P1_0 - P1_{max}}{\omega_0 - \omega_{min}}\right)(\omega_0 - \omega_{island})$$

if

$$P1_0 - \left(\frac{P1_0 - P1_{max}}{\omega_0 - \omega_{min}}\right)(\omega_0 - \omega_{island}) > P1_{min};$$

and wherein

-continued

$$P1_{island} \approx P1_{min}$$

if

$$P1_0 - \left(\frac{P1_0 - P1_{max}}{\omega_0 - \omega_{min}}\right)(\omega_0 - \omega_{island}) \leq P1_{min}.$$

7. The method of claim **6**, wherein the microsource includes power storage such that $P\mathbf{1}_{min}<0$.

8. The method of claim **1**, further comprising:

providing a second microsource, wherein the second microsource is located in the microgrid, and further wherein the second microsource is configured to deliver a power $P\mathbf{2}$ at a frequency $\omega 2$;

operating the second microsource in the grid mode in which the second microsource is connected to the utility grid, wherein during operation in the grid mode, the frequency $\omega 2$ is approximately equal to the frequency ω_o and the power $P\mathbf{2}$ is equal to a power $P\mathbf{2}_o$; and

transferring the second microsource from the grid mode to the island mode such that the second microsource is disconnected from the utility grid, wherein $\omega 2$ is approximately equal to ω_{island} and $P\mathbf{2}$ is equal to $P\mathbf{2}_{island}$ during operation in the island mode;

wherein $\omega_{island}>\omega_o$ and $P\mathbf{2}_{island}<P\mathbf{2}_o$ if the microgrid was exporting power prior to the transfer from the grid mode to the island mode; and

wherein $\omega_{island}<\omega_o$ and $P\mathbf{2}_{island}>P\mathbf{2}_o$ if the microgrid was importing power prior to the transfer from the grid mode to the island mode.

9. The method of claim **8**, wherein $(P\mathbf{1}_{island}-P\mathbf{1}_0)\approx(P\mathbf{2}_{island}-P\mathbf{2}_0)$ such that an amount of change of $P\mathbf{1}$ when the microsource is transferred from the grid mode to the island mode is approximately equal to an amount of change of $P\mathbf{2}$ when the second microsource is transferred from the grid mode to the island mode.

10. The method of claim **8**, further comprising providing a power slope m, and wherein $\omega_{island}\approx\omega_0-m(P\mathbf{1}_0-P\mathbf{1}_{island})\approx\omega_0-m(P\mathbf{2}_0-P\mathbf{2}_{island})$.

11. The method of claim **8**, further comprising providing a power slope m, wherein the microsource has a minimum operating frequency ωmin, wherein $\omega_{island}\approx\omega_0-m(P\mathbf{1}_0-P\mathbf{1}_{island})>\omega_{min}$; and

wherein $\omega_{island}\approx\omega_{min}$ if $\omega_0-m\,(P\mathbf{1}_0-P\mathbf{1}_{island})\leqq\omega_{min}$.

12. The method of claim **8**, further comprising providing a power slope m, wherein the microsource has a maximum operating frequency ω_{max}, wherein $\omega_{island}\approx\omega_0-m(P\mathbf{1}_0-P\mathbf{1}_{island})>\omega_{max}$; and

wherein $\omega_{island}\approx\omega_{max}$ if $\omega_0-m(P\mathbf{1}_0-P\mathbf{1}_{island})\leqq\omega_{max}$.

13. The method of claim **8**, further comprising providing a power slope m, wherein the microsource has a minimum operating frequency ω_{min} and a maximum operating frequency ω_{max}, wherein $\omega_{island}\approx_{min}$ if $\omega-m(P\mathbf{1}_0-P\mathbf{1}_{island})\leqq\omega_{min}$wherein $\omega_{island}\approx\omega_{max}-m(P\mathbf{1}_0-P\mathbf{1}_{island})>\omega_{min}$; and

wherein $\omega_{island}\approx\omega_{max}$ if $\omega_0-m\,(P\mathbf{1}_0-P\mathbf{1}_{island})\leqq\omega_{max}$.

14. The method of claim **1**, wherein the microsource has a maximum power output level $P\mathbf{1}_{max}$, a minimum power output level $P\mathbf{1}_{min}$, and a minimum operating frequency ω_{min}, and wherein

$$\omega_{island} \approx \omega_0 - \left(\frac{\omega_0 - \omega_{min}}{P1_{min} - P1_{max}}\right)(P1_0 - P1_{island}).$$

15. The method of claim **1**, wherein the microsource has a maximum power output level $P1_{max}$, a minimum power output level $P1_{min}$, and a minimum operating frequency ω_{min},

Wherein

$$P1_{island} \approx P1_0 - \left(\frac{P1_{min} - P1_{max}}{\omega_0 - \omega_{min}}\right)(\omega_0 - \omega_{island})$$

if

$$P1_0 - \left(\frac{P1_{min} - P1_{max}}{\omega_0 - \omega_{min}}\right)(\omega_0 - \omega_{island}) > P1_{min}$$

and wherein

$$P1_{island} \approx P1_{min}$$

if

$$P1_0 - \left(\frac{P1_{min} - P1_{max}}{\omega_0 - \omega_{min}}\right)(\omega_0 - \omega_{island}) \le P1_{min}.$$

16. The method of claim **1**, wherein the microsource has a maximum power output level $P1_{max}$, a minimum power output level $P1_{min}$, and a minimum operating frequency ω_{min},

wherein

$$P1_{island} \approx P1_0 - \left(\frac{P1_{min} - P1_{max}}{\omega_0 - \omega_{min}}\right)(\omega_0 - \omega_{island})$$

if

$$P1_0 - \left(\frac{P1_{min} - P1_{max}}{\omega_0 - \omega_{min}}\right)(\omega_0 - \omega_{island}) < P1_{max}$$

and wherein

$$P1_{island} \approx P1_{max}$$

if

$$P1_0 - \left(\frac{P1_{min} - P1_{max}}{\omega_0 - \omega_{min}}\right)(\omega_0 - \omega_{island}) \le P1_{max}.$$

17. The method of claim **1** wherein the microsource has a maximum power output level $P1_{max}$, a minimum power output level $P1_{min}$, and a minimum operating frequency ω_{min},

wherein

$$P1_{island} \approx P1_{min}$$

if

$$P1_0 - \left(\frac{P1_{min} - P1_{max}}{\omega_0 - \omega_{min}}\right)(\omega_0 - \omega_{island}) \le P1_{\min};$$

wherein

$$P1_{island} \approx P1_0 - \left(\frac{P1_{min} - P1_{max}}{\omega_0 - \omega_{min}}\right)(\omega_0 - \omega_{island})$$

if

$$P1_{min} < P1_0 - \left(\frac{P1_{min} - P1_{max}}{\omega_0 - \omega_{min}}\right)(\omega_0 - \omega_{island}) < P1_{max};$$

and wherein

-continued

$$P1_{island} \approx P1_{max}$$

if

$$P1_0 - \left(\frac{P1_{min} - P1_{max}}{\omega_0 - \omega_{min}}\right)(\omega_0 - \omega_{island}) \ge P1_{max}.$$

18. A microgrid comprising:

a microsource comprising a power controller configured to
- control a frequency $\omega 1$ and a power **P1** of the microsource;
- operate the microsource in a grid mode in which the microsource is connected to a utility grid, and wherein the frequency $\omega\mathbf{1}$ is approximately equal to an operating frequency ω_o of the utility grid and the power P1 is equal to $P\mathbf{1}_o$; and
- transfer the microsource to operate in an island mode in which the microsource is disconnected from the utility grid, wherein the frequency $\omega 1$ is equal to ω_{island} and the power P1 is equal to $P\mathbf{1}_{island}$ in the island mode;

wherein $\omega_{island} > \omega_0$, and $P1_{island} < P1_0$ if the microgrid was exporting power prior to the transfer from the grid mode to the island mode;

wherein $\omega_{island} < \omega_0$, and $P1_{island} > P\mathbf{1}_0$ if the microgrid was importing power prior to the transfer from the grid mode to the island mode; and

wherein the microsource delivers a maximum power output level $P\mathbf{1}_{max}$ at a frequency ω_{min}, wherein the microsource has a slope switch frequency ω_{switch}, wherein

$$\omega_{island} \approx \omega_0 - \left(\frac{\omega_0 - \omega_{\min}}{P1_0 - P1_{\max}}\right)(P1_0 - P1_{island})$$

if

$$\left[\omega_0 - \left(\frac{\omega_0 - \omega_{\min}}{P1_0 - P1_{\max}}\right)(P1_0 - P1_{island})\right] < \omega_{switch};$$

19. The microgrid of claim **18**, wherein the microsource delivers a maximum power output level $P1_{max}$ at a frequency ω_{min}, and wherein

$$\omega_{island} \approx \omega_0 - \left(\frac{\omega_0 - \omega_{min}}{P2_0 - P2_{max}}\right)(P2_0 - P2_{island}).$$

20. The microgrid of claim **18**,

wherein

$$\omega_{island} < \omega_0 - \left(\frac{\omega_0 - \omega_{min}}{P1_0 - P1_{max}}\right)(P1_0 - P1_{island})$$

$$\text{if } \left[\omega_0 - \left(\frac{\omega_0 - \omega_{min}}{P1_0 - P1_{max}}\right)(P1_0 - P1_{island})\right] \ge \omega_{switch}.$$

21. The microgrid of claim **18**, wherein the microsource delivers a maximum power output level $P1_{max}$ at a frequency ω_{min}, wherein the microsource has a slope switch frequency ω_{switch}, wherein the microsource has a maximum operating frequency ω_{max}, wherein

$$\omega_{island} \approx \omega_0 - \left(\frac{\omega_0 - \omega_{min}}{P1_0 - P1_{max}}\right)(P1_0 - P1_{island})$$

$$\text{if } \left[\omega_0 - \left(\frac{\omega_0 - \omega_{min}}{P1_0 - P1_{max}}\right)(P1_0 - P1_{island})\right] < \omega_{switch};$$

wherein

$$\omega_{island} < \omega_0 - \left(\frac{\omega_0 - \omega_{min}}{P1_0 - P1_{max}}\right)(P1_0 - P1_{island})$$

$$\text{if } \omega_{switch} \le \left[\omega_0 - \left(\frac{\omega_0 - \omega_{min}}{P1_0 - P1_{max}}\right)(P1_0 - P1_{island})\right] < \omega_{max};$$

wherein

$$\omega_{island} \approx \omega_{max} \text{ if } \left[\omega_0 - \left(\frac{\omega_0 - \omega_{min}}{P1_0 - P1_{max}}\right)(P1_0 - P1_{island})\right] \ge \omega_{max}.$$

22. The microgrid of claim **18**, wherein the microsource delivers a maximum power output level $P1_{max}$ at a frequency ω_{min}, wherein the microsource has a minimum power output level $P1_{min}$,

wherein

$$P1_{island} \approx P1_0 - \left(\frac{P1_0 - P1_{max}}{\omega_0 - \omega_{min}}\right)(\omega_0 - \omega_{island})$$

$$\text{if } P1_0 - \left(\frac{P1_0 - P1_{max}}{\omega_0 - \omega_{min}}\right)(\omega_0 - \omega_{island}) > P1_{min}; \text{ and}$$

wherein

$$P1_{island} \approx P1_{min} \text{ if } P1_0 - \left(\frac{P1_0 - P1_{max}}{\omega_0 - \omega_{min}}\right)(\omega_0 - \omega_{island}) \le P1_{min}.$$

23. The microgrid of claim **22**, wherein the microsource further comprises a power storage unit such that $P1_{min}<0$.

24. The microgrid of claim **18**, wherein the microsource has a maximum power output level $P1_{max}$, a minim urn power output level $P1_{min}$, and a minimum operating frequency ω_{min}, and wherein

$$\omega_{island} \approx \omega_0 - \left(\frac{\omega_0 - \omega_{min}}{P1_{min} - P1_{max}}\right)(P1_0 - P1_{island}).$$

25. The microgrid of claim **18**, wherein the microsource has a maximum power output level $P1_{max}$, a minimum power output level $P1_{min}$, and a minimum operating frequency ω_{min},

$$P1_{island} \approx P1_0 - \left(\frac{P1_{min} - P1_{max}}{\omega_0 - \omega_{min}}\right)(\omega_0 - \omega_{island})$$

$$\text{if } P1_0 - \left(\frac{P1_{min} - P1_{max}}{\omega_0 - \omega_{min}}\right)(\omega_0 - \omega_{island}) > P1_{min};$$

and wherein

$$P1_{island} \approx P1_{min}$$

if

$$P1_0 - \left(\frac{P1_{min} - P1_{max}}{\omega_0 - \omega_{min}}\right)(\omega_0 - \omega_{island}) \le P1_{min}.$$

26. The microgrid of claim **25**, wherein the microsource further comprises a power storage unit such that $P1_{min}<0$.

27. The microgrid of claim **18**, wherein the microsource has a maximum power output level $P1_{max}$, a minimum power output level $P1_{min}$, and a minimum operating frequency ω_{min},

$$P1_{island} \approx P1_0 - \left(\frac{P1_{\min} - P1_{max}}{\omega_0 - \omega_{min}}\right)(\omega_0 - \omega_{island})$$

$$\text{if } P1_0 - \left(\frac{P1_{min} - P1_{\max}}{\omega_0 - \omega_{min}}\right)(\omega_0 - \omega_{island}) < P1_{max};$$

and wherein

$$P1_{island} \approx P1_{max}$$

if

$$P1_0 - \left(\frac{P1_{min} - P1_{max}}{\omega_0 - \omega_{min}}\right)(\omega_0 - \omega_{island}) \ge P1_{max}.$$

* * * * *